Univerzita Karlova v Praze

Přírodovědecká fakulta

Studijní program:

Fyzická geografie a geoekologie

Ye Su

Hydrological processes and dynamics in the changing climate and environment: Lessons learned from multiple temporal and spatial scales

Hydrologické procesy a jejich dynamika v měnícím se klimatu a prostředí: Zkušenosti z výzkumu na různých časových a prostorových škálách

Disertační práce

Vedoucí závěrečné práce/Školitel: Prof. RNDr. Jakub Langhammer, Ph.D.

Praha, 2019

To Sula

Prohlášení:

Prohlašuji, že jsem závěrečnou práci zpracoval/a samostatně a že jsem uvedl/a všechny použité informační zdroje a literaturu. Tato práce ani její podstatná část nebyla předložena k získání jiného nebo stejného akademického titulu.

Declaration:

I hereby declare that I have worked on the final thesis independently and I have reported all the data sources and literature used. This work has not been submitted to obtain any other academic title.

V Praze, 1.8.2019

Podpis/signiture

ACKNOWLEDGEMENT

Sitting in the office, I am recalling all my memories during the period of my Ph.D. study. When I decided to start pursuing my Ph.D. in Charles University in Prague, the journey of my life has turned to a totally different direction – I believe it was and will be one of the most important and good choices I made. I am eternally grateful to my supervisor Prof. Jakub Langhammer for the great opportunities you have provided to me. Your trust in my research competence and your respect for my research interests made who I am now. I gained tons of information during the annual workshops you organized and enjoyed follow-up “party time” with all colleagues a lot. As the first international student in our “hydroteam” as well as in our department, I have received countless help and support from all team members and staffs. I would not complete my study without all of you. Special thank goes to Václav Treml for helping me with institutional paperwork and guiding me to know the department and daily life in Prague. I extend the most sincere gratitude to Michal Jeníček, Lukáš Vlček, Theodora Lendzioch, and Jana Bernsteinová, you are all more than colleagues but friends to me. Thanks for sharing all your knowledge with me and supporting my research whenever I needed you. I enjoyed talking about our research and gossips while drinking the Czech beer or Czech wine.

I would not forget to address my appreciation for the opportunities of collaboration with the other co-authors outside the department, Jerker Jarsjö, and Wei Shao. Jerker Jarsjö, you are my lifelong supervisor in academia who always gives me encouragement and guidance in my research. Thank you for visiting me here in Prague far away from Sweden, I can still remember the time that we sat in the same office in Prague and exchanged ideas by typing words out, which was such an inspiration and fun working process. Wei Shao, you are a good friend who always generously shares experience and knowledge, and is always very effective as a co-author when we worked together. I have to say that we helped each other to be a better researcher. Have Five!

My thanks go to all my family members, especially Ning Zhang, who supported me to accomplish my thesis. You all experienced my ups-and-downs but still love me. During my Ph.D. period, Sula becomes my greatest accomplishment and she enjoyed “reading” scientific paper while taking a nap or sleeping. Sula might be a scientist in the future as she has read many papers at an early age. I am submitting the thesis on the international children’s day as a gift to you and wish you will keep your curiosity to nature where is hidden numerous knowledge, and embrace the fascinating uncertainties in the world.

I am more than certain that these years were the most precious time I ever had. Thank you all for being aside with me.

In Prague 2,

1,6, 2019

Hydrological processes and dynamics in the changing climate and environment: Lessons learned from multiple temporal and spatial scales

Ye Su

ABSTRACT

Climate change, along with the changes in land use and land cover (LULC), is the key factor driving the changes in hydrological processes and dynamics in a basin. This thesis emphasized on understanding the impact of both long-term climate change and abrupt anthropogenic driven agricultural intensification or natural driven insect-induced forest disturbance on hydrological processes and dynamics at varying spatial and temporal scales in two diverting terrestrial environment.

Two pattern-based investigations, one case study in a forest region in Central Europe and another in a semi-arid region in Central Asia, were aimed to answer the main research question "*what are the responses of hydrological dynamics and the related hydro-geochemical conditions to climate change and certain changes in LULC at a basin-scale?*". The long-term hydro-climatic dataset was used for conducting statistical analyses and establishing hydro-climatic modelling at the basin scale. We further conducted process-based studies, attempting to understand how and why the specific hydrological dynamics were altered at smaller spatial and temporal scales: (i) a catchment-scale tracer-based experiment was conducted to examine multi-timescales changes in subsurface chemical composition and in runoff generation processes after bark beetle infestation; (ii) a soil column-scale theoretical analysis was studied to address the importance of velocity-celerity difference in studying tracer transport; (iii) two plot-scale model-based evapotranspiration estimations in a Soil-Vegetation-Atmosphere-Transfer (SVAT) model scheme were conducted to offer an alternative to better understand evaporation from soil, transpiration, and evaporation from canopy; and (iv) a plot-scale sap flow experiment was designed to estimate the canopy conductance during the vegetation period of beech forest.

Two pattern-based case studies pointed out the significant hydrological responses to the warmer climate under different environment, in the studied mid-latitude Central Europe Mountain the runoff seasonality shifted in terms of total runoff share, occurrence of peak flows and low flows, while Central Asia experienced a decrease in river flow and significant changes in riverine nitrogen concentrations. The processes-based studies highlighted that complex hydrological processes including streamflow, subsurface flow, geochemical conditions, and evapotranspiration are actively interacting with the changes in climate and LULC. In the experimental catchments of Central Europe undergone climate-induced bark beetle infestation, the geochemical changes, showing as an increased annual mean in-stream electrical conductivity (EC), are profound in the disturbed catchments were rapid after extensive infestation and last long over decades. The old water with substances of nitrogen and carbon released by dead trees was mixing with the rainwater in the rainfall-runoff events, and the shifts in EC-discharge

hysteresis loops at each event implied changes in the subsurface chemical composition and runoff generation process. Such tracer-related studies require deep understanding in subsurface flow, we, therefore, proposed a celerity function that has been theoretically proved the usefulness when assists in studying runoff behaviours and tracer transport.

Furthermore, evapotranspiration in the forested region is a key domain in the hydrological cycle. The newly developed SVAT model was applied in two different environments (i.e., forest and maize) where had full sets of dataset for validating the model, and the performance was better due to the more detailed description of energy transfer and the formation of advective soil vapour transport. One step forward, the results from sap flow experiment tracked the transpiration process in the beech forest, based on which the reversely-calculated canopy conductance was given to address the importance of knowing the site/species-specific canopy conductance for an area, which assists better understanding the transpiration process in newly formed beech stands after bark beetle outbreak in Central Europe.

Key words: hydrological processes, runoff, climate change, agricultural intensification, forest disturbance, geochemical transformation, celerity, evapotranspiration, SVAT model, sap flow, stomatal conductance

CONTENTS

1. SCOPE AND AIM OF THE THESIS

Studying hydrological processes and dynamics requires multi-disciplinary knowledge, which is also crucial to the environmental managers and planners (Jørgensen, 2016). The scientific information on interactions of a climate-hydrology-ecosystem could be either used to diminish the environmental risks via effective measures or to manage natural resources through more sustainable strategies (Zalewski, 2002). Climate change, along with the changes in land use and land cover (LULC), is the key factor driving the changes in hydrological processes and dynamics in a basin. Both long-term climate change and abrupt anthropogenic or natural disturbance may result in significant shifts in hydrological behaviours, further influencing its hydro-geochemical conditions in the basin.

This thesis, therefore, examined the hydrological processes and dynamics under different environment at varying spatial and temporal scales. For this purpose, two types of LULC change were selected: one is a basin undergone **natural disturbance** (bark beetle infestation) in a **mid-mountain forested region**, and another one is a basin undergone **anthropogenic disturbance** (agricultural intensification) in a **semi-arid irrigated region**. Two study areas are all in the terrestrial environment, and have diverting environmental problems but sharing one same driver – climate change, which could lead to additional changes in multiple elements of the hydrological system. Based on these two diverting study areas, the specific research question is:

> **What are the responses of hydrological dynamics and the related hydro-geochemical conditions to climate change and certain changes in LULC at a basin scale?**

Specifically, for studying the natural disturbance in the mid-mountain forested environment, the study area placed in the upper Vydra basin, the Czech Republic, where experienced the abrupt insect-induced forest mortality in the past 30 years. A study was conducted to statistically assess the historical hydro-climatic changes in the attempting to investigate below research questions:

- What specific runoff behaviours are sensitive to climate change and natural forest disturbance?
- What hydro-climatic indicators are suitable for detecting the extent and timing of such changes?

For studying the anthropogenic disturbance in a semi-arid irrigated region, the example case of the large (covering 1.3% of the earth's land surface) and extensively irrigated Aral Sea Drainage Basin (ASDB) in Central Asia was used. The historical hydro-climatic conditions in ASDB experienced dramatic changes due to both climate change and irrigation practices. The agricultural intensification area was convinced to be highly sensitive to future climate change (Törnqvist et al., 2015). A study was conducted aiming to use the multiple climate change scenarios to model possible runoff and its related retention–attenuation of nutrient, and answering the research question:

- What are the dynamics between future climate projections and runoff variations?
- To what extent the projected future climate change and runoff can influence nitrogen loads and concentrations in the water systems of the basin?

Though in the environment has relatively limited anthropogenic interventions, the land cover could still be altered by the changing climate, in the example of bark beetle infestation illustrating the growth of beetle populations respond to the shifts in thermal condition and water stress (Anderegg et al., 2015; Bentz et al., 2010). Therefore, the projected climate warming and changing precipitation patterns could pose high future risks of infestation (Berg et al., 2006; Williams et al., 2013). In one of our key study sites, the upper Vydra basin has been experienced such risk. We examined the long term basin-scale hydro-climatic changes, and further aimed to scale down to its nested catchments, and investigated its possible hydrological and geochemical responses at the smaller spatial scale.

The nested catchments experienced different stages of forest disturbance, we tracked the temporal dynamics over 7 years in each individual catchment using our monitoring network. The electrical conductivity (EC) was chosen to be the geochemical parameter reflecting the changes in water flow paths. In addition, we traded time for space in understanding the processes of forest decay, degradation, and regeneration in response to streamflow and geochemical conditions. The below-given research questions were formulated:

- What extent does the bark beetle-induced forest disturbance alter geochemical conditions in small catchments at multiple timescales?
- And what are the runoff generation mechanisms before and after the insect infestation?

Understanding the implications from the above tracer-based study are important due to its complicity. The complex solute transport behaviours are caused by the pore water velocity distribution in the subsurface flow system (Beven and Germann, 1982; Freer *et al.*, 2002; Uchida *et al.*, 2004), which have been captured either by an experimentally-obtained breakthrough curve (Brusseau and Rao, 1990; Durner and Flühler, 1996; Flühler *et al.*, 1996) or by natural and artificial tracers in a hydrological system (Kendall *et al.*, 1999; Köhne *et al.*, 2009). Therefore, theoretical analyses were conducted to assist in understanding the implications of the tracers in hydrological studies and how to accurately interpret tracer transport together with water flow, in which the research question was mainly dealing with:

- What are the relations between celerity (pressure propagation), velocity (water transport), and tracer transport (pore velocity distribution)?
- What soil hydraulic function could be used to express the tracer transport?

This thesis started from understanding of the changes in hydrological patterns narrowing down to investigate the specific hydrological processes. Climate change may cause variations on metrological forcing of precipitation, air temperature, radiation, air humidity, and wind speed, while, ecosystem change or human activity may affect the LAI, stomata behaviours, albedo, surface roughness, and soil hydraulic properties. All changing variables in the system interact and are related to the evapotranspiration processes. Therefore, quantifications of evapotranspiration rate and understanding the evapotranspiration process are critical to study how and why the hydrological dynamics were shifted or changed under the changing environment.

We here firstly developed a new numerical model, which simulated both energy and moisture transport in a soil–vegetation–atmosphere transfer continuum, being named as an SVAT model. The model developed by incorporating theories from soil physics, vegetation physiology, and atmospheric science (Gran et al., 2011; Overgaard et al., 2006), and tested in two types of vegetated area where had comprehensive monitoring dataset of water and energy fluxes that can validate its utility and accuracy. Thereafter a sap flow experiment, along with soil profile monitoring, was carried out in one experimental plot at one of the nested small catchments in the upper Vydra basin. The 3-month high-frequent measurements enabling us to investigate quantify the transpiration process in Century European mid-mountain beech forest on a more detailed level and the following questions were set up for the research.

- How the evapotranspiration rates can be quantified in the forested area using only meteorological data?
- What is transpiration behaviour of mountain beech forest in the study area?

2. RELEVANCE AND BACKGROUND OF THE THESIS

2.1 Climate change and relevant hydrological responses

Five Intergovernmental Panel on Climate Change (IPCC) assessment reports together presented a piece of clear evidence – global temperature warming (IPCC, 2007; IPCC, 2013). The recent IPCC (2013) report stated that a global mean surface temperature rise of approximately 0.85°C (ranging from 0.65°C to 1.06 °C) over the period 1880–2012 (IPCC, 2007; IPCC, 2013).

The past climate signals and the knowledge of the system's physical feedbacks and behaviours enable re-analysing the past and future climate in more detail by using climate circulation models (Christensen *et al.*, 2007; Nicótina *et al.*, 2008). The models used plausible physical processes embedded with a large variety of physical, chemical, and biological mechanisms and processes to represent energy and water fluxes across atmosphere, water, vegetation, and land surface (Hornbeck *et al.*, 1970). Though the accuracy of climate change predictions is still questionable due to large uncertainties derived from such complicated models (Kriaučiūnien *et al.*, 2009; IPCC, 2013), a rather confident message can be gained from many publications, for instance, a recently published IPCC report (IPCC, 2013) predicted that the annual mean temperature was likely to continuously increase, yielding a total increase between the range 0.3°C and 4.8°C (based on a recently published set of greenhouse gas (GHG) emission scenarios) by 2100 in comparison with the period of 1986 - 2005.

Along with the increasing air temperature, climate change associates with the changes in global mean water vapour, precipitation and evapotranspiration rates, the variations show large differences in space (IPCC, 2013). Theoretically, warmer air implies a higher evaporation rate and a greater proportion of liquid to solid precipitation. Such changes in physical mechanisms are associated with potential changes in precipitation amount and seasonality, and particularly in spatial distribution of the precipitation. For instance, in Central Asia, the observed mean annual precipitation has increased in outer and eastern ranges, while decreased at higher altitudes in the inner ranges (Sorg *et al.*, 2012). The changes in precipitation in turn affect directly or indirectly water availability (in terms of soil moisture and groundwater reserves) and streamflow regime (in terms of pattern, magnitude, frequency of flood or drought episodes, timing, duration and change rate) (H.Gleick, 1989; Dam, 1999; Barnett *et al.*, 2005; Milly *et al.*, 2005).

In recent decades, the understanding of the climate change shifted from a simplified cause-effect approach to a feedback-oriented approach for modelling the system (Sklash *et al.*, 1986; Eltahir, 1998). The improvement in understanding of the feedback system and climate sensitivity moves the projection towards better simulating how human activities will be developed under different conditions to respond to the changing climate (Manabe and Stouffer, 1980; IPCC, 2013; Voldoire *et al.*, 2013). No matter in physical or social aspects regarding climate change, the plausible climate change projections and the analyses of its effects are considered as an important basis for future regional development planning (Milly *et al.*, 2005).

Climate change will have a range of consequences at different spatial and temporal scales which will impact hydrological processes. Basin-scale studies were conducted worldwide aiming to obtain more profound understanding of climate change impacts under each specific regional environment. Studies found that the largest and the most sensitive changes in the hydrologic cycle are expected to occur in mid- to high-latitude snow-dominated mountainous regions (Barnett *et al.*, 2005), and in arid and semi-arid regions (Lioubimtseva and Henebry, 2009; Jarsjö, 2012; Sorg *et al.*, 2012), respectively.

In a snow-dominated mountainous basin, the hydrologic responses to climate warmer summarized as the changes in the runoff timing associated with reduced snowpack accumulation and earlier melting time (Beniston, 2003; Eckhardt and Ulbrich, 2003; Adam *et al.*, 2009). The melting influences discharge rates and timing in the rivers that originate in mountains, therefore, shifts in snow-pack duration and amount as a consequence of climate change will be crucial factors in water availability for basins (Beniston, 2003). The consequences for river runoff are likely to affect not only the basin itself, but also in the lowland regions especially when the extreme events (floods or drought) occur. In summer, mean monthly groundwater recharge and streamflow are likely to reduce dramatically in the basin which could potentially lead to problems for the whole region concerning water quality, groundwater withdrawals, and functionality of reservoirs (Eckhardt and Ulbrich, 2003). Even though the snow-dominated mountainous basin share similar trends, each basin characterized by its geophysical conditions owning individual responses to the changing climate, Langhammer *et al.* (2015) provided additional inputs for understanding the impact of climate change to runoff regimes in such an environment.

In a semi-arid basin, shrinkage of the Aral Sea in the past century is a shred of alerting evidence that states the combination of elevated temperature and decreased precipitation could cause a manifold increase in potential evapotranspiration, leading to severe water stress conditions and reduction on river discharge in the outlet (Arora and Boer, 2001; IPCC, 2007; Micklin, 2007; Shibuo *et al.*, 2007). IPCC (2013) revealed that the frequency and severity of extreme events would rise. Taken together, as the current marginality of soil-water and nutrient reserves has reached their tolerances, some ecosystems in semi-arid regions may be among the first to show the effects of climate change. In the Aral Sea Drainage Basin (ASDB), most of the croplands are open-channel irrigated due to low and highly variable rainfall, therefore, the evaporation loss will increase under warmer climate (Törnqvist and Jarsjö, 2012). Therefore, understanding the future trend of river runoff in the entire basin, in particular in the lowland areas, was crucial for regional planning and water resource management.

2.2 LULC change and its hydrological responses under changing climate

Change in land cover stemming from land uses represents either a major source or a major element of global environmental change (Turner *et al.*, 1994). LULC is defined by the attributes of the earth's land surface and immediate subsurface, including biota, soil, topography, surface and groundwater, and human structures (Lambin *et al.*, 2003). The magnitude of changes in LULC is large over the past century, which significantly affects the functionality of the Earth system. Moreover, LULC change, in turn, contributes to local and regional climate change as well as to global climate warming (Houghton, 1999; Pielke, 2005). Feddema *et al.* (2005) found through models that the future LULC will most likely continue to be an important influence on climate for the next century. This finding opens new possibilities for modelling climate change by adding the accurate full range of phenomena caused by LULC changes.

Most current research tracks under this topic were mainly focused on studying the interactions between climate change and the changes in vegetation cover (Matthews, 1983; Stow *et al.*, 2004), agricultural intensification (Tilman, 1999; Shibuo *et al.*, 2007), and urbanization (Carlson and Arthur, 2000; Kalnay and Cai, 2003). Furthermore, studies on exploring the LULC on either systematic global environmental changes (e.g., changes in bio-geo-chemical circles and climatic variation), or cumulative global environmental changes (e.g., deforestation, biodiversity reduction, and land/soil degradation) are also been recognized as important research directions (Lambin *et al.*, 2003). Natural landscape transitions or anthropogenic changes are affected together under climate change, and many studies (Birsan *et al.*, 2005; Ma *et al.*, 2010; Ahmad *et al.*, 2012; Zhang and Wei, 2012) pointed out both long-term and abrupt changes may result in significant shifts in runoff regime, especially in response to extreme runoff events like floods and droughts. In such a complex system, the understanding of each hydrological domain under different environment is vital to the whole picture towards global perspective. The river is increasingly investigated as a landscape itself (Robinson *et al.*, 2002) and as an ecosystem that is strongly influenced by their surroundings through which they flow at multiple scales (Allan, 2004).

Forest disturbance is the most significant drivers of land cover changes, in particular in a montane environment with coniferous forest and the boreal forest, the vulnerability of forest disturbances is highly linked to the increasingly warmer and drier climate (Seidl *et al.*, 2017). Except for the natural processes, agricultural intensification is one of the key anthropogenic land-use processes influencing the regional environment, in particular in the semi-arid area where has a large-scaled irrigation system. Such land use is convinced to be highly sensitive to future climate change (Jarsjö *et al.*, 2012). Therefore, two main LULC types were emphasized below for detailed reviews.

2.2.1 Forest disturbance

Forest disturbance is one of the causes of driving severe land cover change, which has strong impacts on rainfall interception, evapotranspiration, surface soil hydraulic conductivity and soil storage which consequently results in changes in the runoff formation process and basin water yields (Bosch and Hewlett, 1982; Buttle and Metcalfe, 2000; Beudert *et al.*, 2007; Pomeroy *et al.*, 2012).

Climate change, namely increasing air temperature and changing precipitation, can affect forests through altering occurrence, timing, frequency, duration, extent, and intensity of various natural disturbances, including fire, drought, introduced species, insect and pathogen outbreaks, storms (e.g., hurricanes, windstorms, and ice storms), or landslides (Dale *et al.*, 2001). Except for the climate-driven factors, logging (Hill *et al.*, 1995), pollution (Gundersen *et al.*, 2006), urbanization (Browder, 2002), agricultural activities (Grau *et al.*, 2005) and environmental management options (Kaimowitz, 1996) are also the common causal factors of forest disturbance. The insect-induced forest disturbance is one of the most sensitive disturbance to the changing climate, which is largely controlled by thermal variation and water stresses (Berg *et al.*, 2006; Bentz *et al.*, 2010; Williams *et al.*, 2013).

From the eco-biological perspective, a recent synthesis of historical data from the southwestern United States showed that the increasing air temperature is related to increase forest drought stress, tree mortality, and large bark-beetle outbreaks (Williams *et al.*, 2013). Furthermore, considering current projections of continued climate warming, there are apparent risks of movements northward and towards higher elevations of bark beetle species that currently are limited by climatic conditions (Bentz *et al.*, 2010). The prolongation of the warm season can also support the second generation of bark beetles (Seidl *et al.*, 2011), and will likely expand the extent of the affected areas. Additionally, until vegetation sufficiently regenerates, infested areas will constitute a carbon source that contributes to increased atmospheric concentrations of carbon dioxide (Kurz *et al.*, 2008). The tree mortality caused by climate change-associated stresses and bark beetle outbreaks poses a significant threat to current forest ecosystems and is emerging as a global concern.

For hydrologists, there is a need to understand and ultimately quantify how potential changes in vegetation structure and function may dampen or amplify changes in the timing and magnitude of streamflow associated with warmer temperatures. Tree devastation commonly impacts the prevailing water balance by decreasing the overall evapotranspiration (Ford and Vose, 2007; Redding *et al.*, 2008; Bearup *et al.*, 2014), causing increases in overland flow or groundwater flow depending on soil infiltration capacity, which results in potentially more water available for streamflow. The soil infiltration capacity can in turn depending on ambient conditions, either be enhanced through the favourable texture of dead material like needle litter from dying trees and through creation of macropores when dead trees fall down (Adams *et al.*, 2012), or be reduced if soil organic material is washed away (Xiong *et al.*, 2011).

Additionally, forest disturbance can affect the geochemical conditions in soil and water, leading for instance to changes in carbon (Kaňa *et al.*, 2013; Reed *et al.*, 2014), nutrient (Huber *et al.*, 2004; Beudert *et al.*, 2007; Mikkelson *et al.*, 2013); and trace metal balances (Bearup *et al.*, 2014). Such changes can be complex, as exemplified by pine forest subjected to insect infestation, and studies (Vitousek *et al.*, 1979; Clow *et al.*, 2011; Edburg *et al.*, 2012; Mikkelson *et al.*, 2013) found common features: nitrogen (N) rich needles initially decay more quickly than the low N high carbon (C) branches, and after the tree dieback, the released N and C from the tree trucks then accumulate in the soil, which acts as a sink, and is available for transport with the subsurface flow, or uptake by the subsequent regenerating forest. Although previous studies provided valuable insight regarding relevant processes, there is still a knowledge gap concerning the implications between different temporal scales regarding potential variations of hydro-geochemical conditions. New understanding could reflect mechanisms behind the accumulative impacts of bark beetle infestations on hydrogeochemical conditions at various temporal scales.

2.2.2 Agriculture intensification

Land use has generally been considered a local environmental issue, but it is becoming a global concern as worldwide changes to forest, agriculture lands, water system, and air are being driven by the need to provide food, fibre, water, and shelter to human beings (Foley *et al.*, 2005). The intensive agriculture largely replies on the renewable water resources, especially in semi-arid and arid regions of South-Eastern Australia (Walker *et al.*, 2009), Central Asia (Shibuo *et al.*, 2007), the Middle-East (Venot and Molle, 2008), Northern Africa (Kotb *et al.*, 2000) and the Western United States (Hauer and Lorang, 2004) are currently diverted and used for irrigation. Meeting irrigation needs of water demanding crops (e.g., rice and cotton) in such extensive agricultural areas largely enhance the water loss through evapotranspiration (ET) by approximately 2 000 km^3/year, which constitutes a majority of the total freshwater consumption (Foley *et al.*, 2005; Shibuo *et al.*, 2007; Jarsjö *et al.*, 2012; Törnqvist and Jarsjö, 2012). Such significant changes could lead to a decrease in runoff and alternations in hydrological conditions and water availability at local, to basin, even to global scales. Particularly, in basins characterized by increasing agricultural water diversions and decreasing runoff, available water must be increasingly recirculated in order to meet irrigation needs (Jarsjö *et al.*, 2017).

Shrinkage and degradation of waterbody are suffering from severe environmental problems such as cruel desiccation, land degradation, desertification, contamination, salinization, and loss of biodiversity. Especially, Central Asia’s closed and terminal lakes are very susceptible to the changes in water balance and the potential changes in this region as a result of two mechanisms- rapidly climatic variability and anthropogenic pressures (Qi and Kulmatov, 2008). Since the 1960s, the large-scale irrigation was implemented to provide water to cotton production in Soviet Central Asia, ever-increasing water withdrawal from the two inflowing rivers, Amu Darya and Syr Darya, has resulted in the dramatic decline of the level, area and volume of the sea (Saiko and Zonn, 2000; Jarsjö *et al.*, 2011; Törnqvist *et al.*, 2011). Over the last 5 decades, the highly managed basin has exacerbated the vulnerability of such arid regions to react even to relatively minor climate variations, particularly in the western parts of Turkmenistan, Uzbekistan, and Kazakhstan (Arora and Boer, 2001; Lioubimtseva and Henebry, 2009; Jarsjö *et al.*, 2011). Under the future climate change, their response to hydrological events is fundamentally changed through regulation (e.g., Palmer et al., 2008), and the spread of water at the land surface through irrigation means that the basin-scale ET and runoff can become considerably more sensitive to changes in average temperature (e.g., Jarsjö et al., 2012).

Changes in LULC and water utilization of the past century have considerably impacted the cycling of water and water-borne substances (Foley *et al.*, 2005; Jarsjö *et al.*, 2017). The intense agriculture in such basins can also considerably contribute to pollutant and nutrient releases of pesticides, herbicides, fungicides and nitrogen, and salt accumulation in agricultural regions worldwide (Foley *et al.*, 2005; Gordon *et al.*, 2008; Törnqvist *et al.*, 2011). Once released, the modified hydrological conditions of managed basins can also fundamentally impact the water-borne transport pathways, travel times, retention-attenuation and discharge of substances into downstream recipients (Palmer *et al.*, 2008). Observations across different scales ranging from laboratory experiments, upscaling to agricultural plots and to hydrological basins show that increasing degree of water recirculation is commonly associated with increasing nutrient attenuation and decreasing downstream nutrient concentration, which may be due to increased nutrient exposure in surface water that can favour nitrogen removal through denitrification, or increased flow path lengths through groundwater systems that can have a filtering effect (Takeda *et al.*, 1997; Feng *et al.*, 2004; Hitomi *et al.*, 2006; Jarsjö *et al.*, 2017). As the decrease in river runoff in the lowland regions affect not only the water cycle, but also the nitrogen circle (Törnqvist *et al.*, 2015), a followed up study was needed to predict the potential change of nitrogen cycle under different climate change scenarios. Such change will limit the access to the suitability of drinking water and post water-borne health risk in the region (Törnqvist *et al.*, 2011), which would be important for many highly managed basis in arid and semi-arid regions of Central Asia and worldwide.

3. PRINCIPAL CONCEPTS AND THEORIES

3.1 Catchment-scale runoff generation

Theories in this chapter was used to obtain a holistic conceptual model for understanding the regional hydrological behaviours. The wide range of runoff generation processes provide a foundation for studying the hydrological processes and behaviours in a basin.

The hydrological system is heterogeneous at all scale, which attributes to the spatial or temporal variations in soil hydraulic properties (Abdul and Gillham, 1989; Zhao *et al.*, 1995; Gannon *et al.*, 2014; Geris *et al.*, 2014), topography (Anderson and Burt, 1978; McGuire *et al.*, 2005), and land use (Bronstert *et al.*, 2002; Bachmair and Weiler, 2012; Muñoz-Villers and McDonnell, 2013). Consequently, the storage and flow velocity in a system expresses a nonlinear behaviour at various scales. Therefore, quantifying and modelling such complex responses of a catchment to various rainfall events require a better understanding of the runoff sources, flow paths, and transit time distributions (Burns *et al.*, 2001; Tetzlaff *et al.*, 2014). Headwater catchment transmits waters to the outlet of stream, processing beyond the permanent stream channel itself (Hewlett and Hibbert, 1967; McDonnell and Beven, 2014).

Classical runoff generation theories explore the contribution of the surface runoff to peak streamflow. The Horton overland flow is triggered by a rainfall intensity threshold, and it is often called infiltration-excess overland flow, which explains during the storm such surface runoff occurs when the rainfall intensity exceeds soil infiltration capacities (Horton, 1933). The Horton overland flow is often used for the semi-arid areas where the storage capacity is difficult to be filled, and the soil permeability is low (Bonell and Gilmour, 1978). While, the Dunne overland flow is triggered by a rainfall magnitude threshold, and it is often called saturation overland flow, which conceptualizes the occurrence of such surface flow is when (or after) a sufficient amount of rainfall filling the soil moisture deficit till saturated (Dunne, 1978). The theory of saturated overland flow has been extensively adopted in conceptual hydrological models, such as TOPMODEL (Beven and Kirkby, 1979), Xinanjiang Model (Zhao, 1992), VIC model (Liang *et al.*, 1994), and FLEXTOP (Savenije, 2010), which suitably simulate the runoff generation in a humid vegetated area where the water storage capacity is low but soil permeability is high.

Recently, it is recognized that the subsurface stormflow (more detailed subsurface flow was described in **Chapter 3.3**) hydraulically links the hillslope (lateral subsurface flow) and riparian area (saturated overland flow) (McGuire *et al.*, 2005; Weiler and McDonnell, 2007). Driven by the hydraulic gradient (Seibert *et al.*, 2003; Weiler *et al.*, 2006), the lateral subsurface flow transports waters through hillslope from near-saturated areas to the riparian area, and supports generating the base flow of a stream (Weiler *et al.*, 2006). However, if the magnitude of rainfall infiltration surpasses a certain threshold, the lateral subsurface flow occurs as the preferential flow via paths with high-permeability, such as macropores or pipes, which significantly and rapidly contributes to the peak streamflow (Weiler *et al.*, 2003; Uchida *et al.*, 2004; Weiler and McDonnell, 2004; Weiler and McDonnell, 2007). Subsurface stormflow may enhance the development of hydraulic connectivity, which most probably occurs in the root zone with abundant preferential flow paths (Uchida *et al.*, 1999; Weiler *et al.*, 2003; Weiler *et al.*, 2006). The infiltration may cause a rapid rise of the water table and an elevation of the capillary fringe to the surface, which yields an increasing fraction of the drainage area to contribute overland flow to the streamflow, and such mechanism is named as "groundwater ridging" (Sklash and Farvolden, 1979; Bonell, 1998).

A general conceptual model of runoff generation for the catchments in Upper Vydra Basin

A conceptual model given here (Fig. 1) is the baseline hypothesis that we adopted for the initial analysis. After the changing LULC, e.g., different stages of bark beetle outbreak, the runoff generation processes slightly altered under different conditions in different catchments.

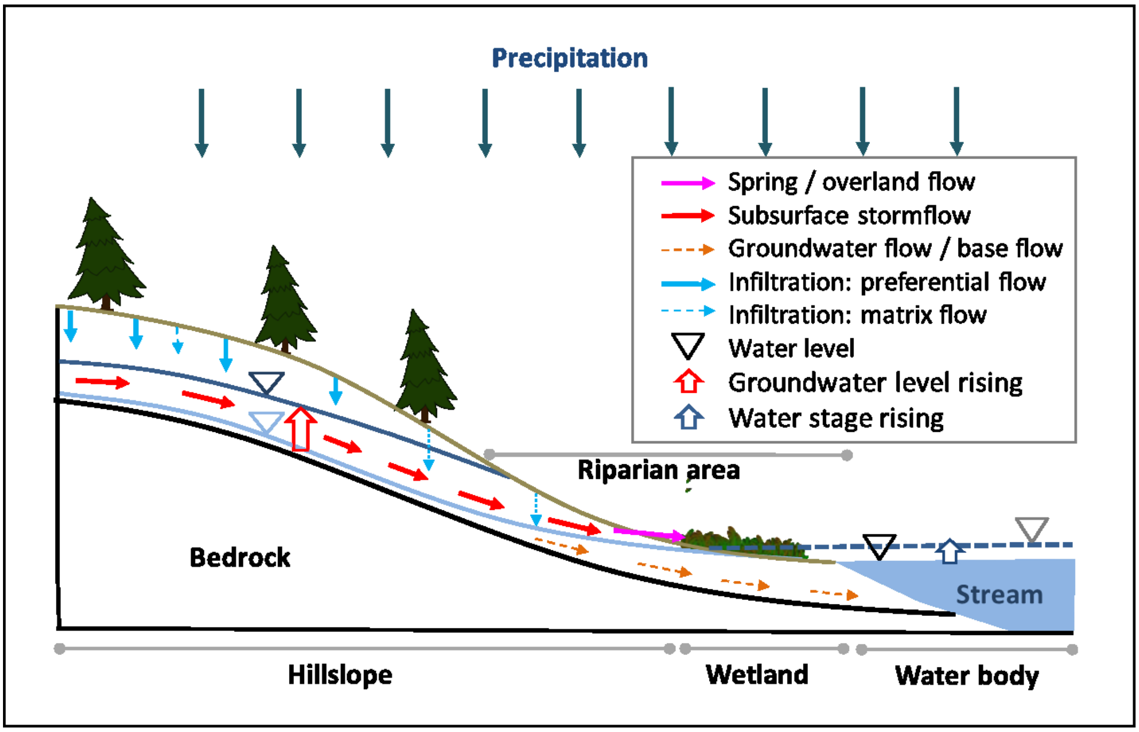

Figure 1. *Conceptual model of the runoff generation for the catchments in the upper Vydra basin.*

- ***Hillslope:*** It is also called uplands, where the groundwater level is commonly below the soil surface. Hillslope is characterized as a hydrological landscape unit transporting energy, materials, and water downgradient to lower areas or a river channel, in the forest headwater catchments, majorly through subsurface flow (Wilson *et al.*, 1990; Bonell, 1998; Uchida *et al.*, 2004; Bachmair and Weiler, 2012). However, the velocity of subsurface flow is depending on the depth of groundwater and the connectivity of flow path (Sklash and Farvolden, 1979; Seibert *et al.*, 2003; Gannon *et al.*, 2014; Tetzlaff *et al.*, 2014). A rise of groundwater may induce an expansion of the saturation area for the following runoff generation from the riparian area or springs in the form of overland flow, under which the water level variation is depending on the drainable porosity of soil porous medium.

- ***Wetland:*** It is a hydrological landscape unit almost maintaining saturation of surface and subsurface water body, where the hydrological response is instant achieved by the transmission of pressure wave, namely, owning a very high celerity. A rising water level in hillslope can instantly cause a volumetric flow increment through the transport the water to the river system. Wetland has a hydrological function of damping the velocity of surface runoff, which provides a transition zone for stormflow to infiltrate the water into the soil (Bullock and Acreman, 1999; Haidary *et al.*, 2013).
- ***Riparian zone***: It is characterized by a high water table, and under different wetness condition along with the rising and falling of saturation and the adjacent water body, the size is subject to expand and shrink (Naiman and Décamps, 1997; Hangen *et al.*, 2001). Riparian areas are an interface of vegetated ecosystems buffering between land and a river or stream, appearing as swamps, marshes, or bogs, among which wetland is a part of area inundated or saturated by surface (ground) water at a frequency and duration sufficient to support the micro-ecosystem (Naiman and Décamps, 1997; Ilhardt *et al.*, 2000).

3.2 Tracer hydrology

The spatial and temporal heterogeneity of the catchment characteristics and hydro-pedagogical conditions make the runoff generation mechanisms hard to be assembled only by localized observation of soil moisture and groundwater (McDonnell, 2003), therefore, the tracers (e.g. chloride, bromide, isotopes, EC, and lithium) are often adopted to differentiate the flow path the resident time of waters in different contributing areas. It is possible to use a tracer to study runoff behaviour considering the different characteristics of new water (i.e., precipitation water) and old water (the water stored in the catchment prior to a hydrologic event) (Pinder and Jones, 1969; Buttle, 1994; Laudon and Slaymaker, 1997; Rice and Hornberger, 1998; Weiler *et al.*, 2003; Blume *et al.*, 2007; Pellerin *et al.*, 2008; Park *et al.*, 2011).

Many tracers experiments found that during a storm event, the old waters in soil and groundwater release to generate the streamflow, while, the event tracer signals also occur in the stream via a "shorter" paths (Phillips, 2010). The infiltration in the soil layer facilitates the mixing process of the event water with the stored pre-event water in the matrix, and the mixed water is successively transported via the preferential flow paths (Uchida *et al.*, 1999; Weiler and McDonnell, 2007). Such mixing process is complicated in hillslopes or riparian area, and also name as an ''effusion confusion'' effect (Weiler and McDonnell, 2007; Phillips, 2010). The physical explanation of such an "old water paradox" needs explicit quantifications of both the threshold behaviours of a contributing area in response to the rainstorm (Bishop *et al.*, 2004; Botter *et al.*, 2010; Phillips, 2010; McDonnell and Beven, 2014; Tetzlaff *et al.*, 2014). Thus, more thorough studies on quantifying the contributing components of runoff generation processes in a catchment in time and space, such as the spatial distribution of riparian areas and hillslopes (Bonell, 1998), and temporal distribution of dry and wet periods.

Although tracking input-output mass and concentration of the conservative tracers remain high uncertainty in the experiments and interpretations, insights on the temporal and spatial tracer movements allow hypothesizing the dominant flow paths and internal mixing processes in/between different land units of/ between (a) catchment(s)(Muñoz-Villers and McDonnell, 2012; Hrachowitz *et al.*, 2013; Tetzlaff *et al.*, 2014). Solute transport in a catchment is often analysed according to a time-variable theory of residence times in a hydrological system due to their high variability in time and space, which largely relies on the high-frequency measurements of in-and-out fluxes on mass and concentration (Botter *et al.*, 2008; Beven, 2010; Botter *et al.*, 2010).

The single-event analysis based upon tracer data is often constrained by nature of the non-linear catchment behaviours and the limitations of the temporal data. Moreover, considering the high analytical costs of isotopes, and the feasibility of using EC as a tracer for hydrograph separation (Pinder and Jones, 1969; Nakamura, 1971; Laudon and Slaymaker, 1997; Moore *et al.*, 2008; Pellerin *et al.*, 2008; Khaledian *et al.*, 2012; Muñoz-Villers and McDonnell, 2012; Zabaleta and Antigüedad, 2013).

3.3 Subsurface hydrology

Subsurface flow is an essential part of the hydrological cycle, in which the infiltration or exfiltration in the vadose zone and groundwater flow are correlated with the evaporation and streamflow generation (Freeze, 1972; Nielsen *et al.*, 1986; Beven, 1989; Kampf and Burges, 2007; Monteith and Unsworth, 2013; Moene and van Dam, 2014).

The Darcy-Richards equation and its simplifications (for sequentially coupling models) are all based on the physical principles of mass and momentum conservation (D'Odorico *et al.*, 2005; Kampf and Burges, 2007), which is frequently coupled with the equations expressing solute transport, thermal transport, and soil mechanics. Such coupling has been widely used to quantify the interaction between water flow and the other physical phenomena in the subsurface flow system (Kampf and Burges, 2007; Cainelli *et al.*, 2012; van Genuchten *et al.*, 2014). However, the physical-based Darcy-Richards equation cannot fully describe the complex phenomena of preferential flow in the heterogonous soil porous medium (Beven and Germann, 1982; Freer *et al.*, 2002; Uchida *et al.*, 2004; Beven and Germann, 2013). The activated preferential flow causes subsurface stormflow in hillslope and catchment after certain saturation or rainfall amount (Uhlenbrook, 2006; Zehe *et al.*, 2010), and contributes a peak flow of the streamflow (Beven, 1981; Uchida *et al.*, 2004; Nieber and Sidle, 2010).

The paradox and threshold behaviour mentioned in previous **Chapter 3.2** may reflect on a bimodal behaviour of the hydrological system, namely, the tracer/solute transport and the streamflow formation are controlled by both of the preferential flow and the matrix flow. Many field studies indicated that the occurrence of preferential flow to the total effective runoff may increase in rainfall magnitude, especially, under the high intensity storm the contribution of preferential flow to the peak subsurface flow may be beyond 90% (Uchida *et al.*, 2001).

The simulation and physical interpretation of subsurface water and tracer transport are necessary to be improved by involving the subsurface flow's velocity and celerity (McDonnell and Beven, 2014). As the celerity mainly describes the pressure wave and fluid wave under a disturbance, it is possible to be mathematically defined and even used as an important indicator to quantitatively describe the various hydraulic behaviours and transport phenomena for multiple scales. The explicit and systematic definition and quantification of velocity and celerity could assist in understanding of the complex transport phenomena and threshold hydrologic behaviours in the subsurface hydrological system.

In general, celerity denotes the velocity of wave prorogation (e.g., heat wave, pressure wave, fluid wave, etc.) induced by a perturbation (i.e. the tiny change of state variable or flux on the boundary) (Singh, 2002). For a block of soil as a simple subsurface flow system, a pressure wave propagation under a perturbation at the surface boundary is following different mechanisms depending on whether the subsurface flow system is confined or not (Fig. 2).

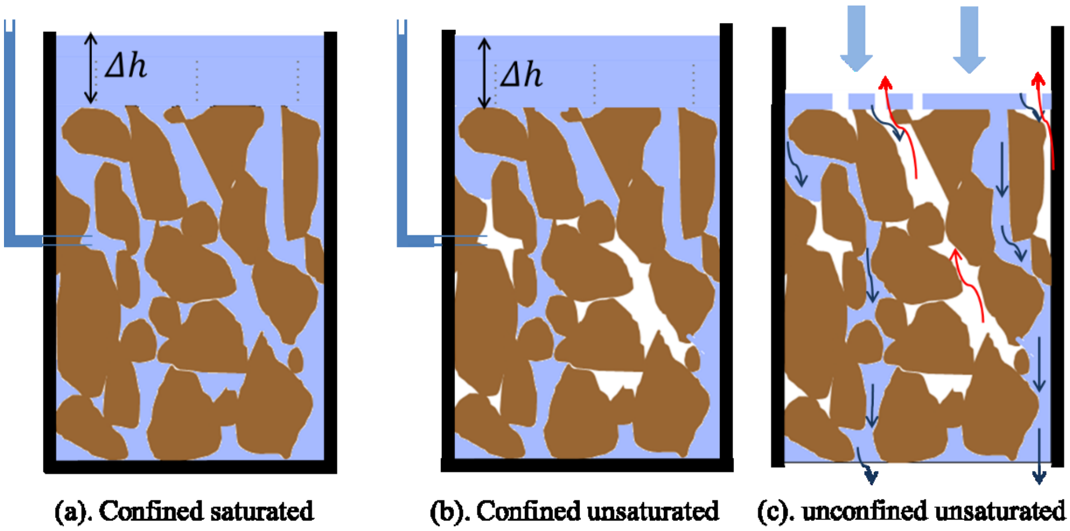

Figure 2. *Conceptual sketch showing the pressure propagation and water flow under an increase of pressure head in the confined and un-confined soil with different saturation states.*

In a confined saturated soil (Fig. 2a), the pressure propagation strongly depends on the compressibility of water and soil porous medium, in which the pressure wave instantaneously emerges without the need to cause an observable water flow. While the occurrence of a pressure wave under an unsaturated state in a confined soil (Fig. 2b) is influenced by entrapped air that cannot freely escape from the porous medium. Such a condition might happen as a special case of ponding infiltration in natural soil, which consequently hampers the infiltration (Wang *et al.*, 1998; Kuang *et al.*, 2013). The compressed air transmits pressure from the ponding surface directly to the deep soil, which causes a fast response on the groundwater table, known as the Lisse effect (Weeks, 2002; Kuang *et al.*, 2013; Waswa *et al.*, 2013). Weeks (2002) concluded that the Lisse effect only happens under an ideally-designed experimental environment. In natural soils, the unsaturated flow generally takes place under an unconfined condition (Fig. 2c). In our study, it is assumed that all air stored in pores can freely escape during an infiltration event. The pressure propagation in such an unsaturated soil can be considered as equivalent to water particle movement. Table 1 listed the equations of velocity and celerity under different conditions.

Table 1. *A summary of three continuity equations for expressing different velocities under various conditions*

Flow types **Flow direction**	**All conditions** **All directions**	**Unsaturated infiltration** **Vertical**	**Unconfined Groundwater flow** **Lateral**	**Saturated flow** **e.g. Vertical**
	Richards	Kinematic Wave	Kinematic Wave	Diffusion Wave
Equation	$\frac{\partial\theta}{\partial t}=\nabla\cdot\left[K(\nabla h+\nabla z)\right]$	$\frac{\partial\theta}{\partial t}=\frac{\partial K}{\partial z}$	$\theta_e\frac{\partial h_B}{\partial t}=K\sin\alpha\frac{\partial h_B}{\partial x}+R$	$S_s\frac{\partial h}{\partial t}=\nabla\cdot\left(K_s\nabla h\right)$
Darcian velocity	$u=-K(\nabla h+\nabla z)$	$u=K_s\Theta^m$	$u=K_s\sin\beta$	$u=K_s\frac{\partial h}{\partial z}$
Average pore velocity	$v=\frac{u}{\theta}$	$v=\frac{u}{\theta-\theta_r}$	$v=\frac{u}{\theta_s}$	$v=\frac{u}{\theta_s}$
Celerity	$c=\frac{dh}{d\theta}\frac{\partial u}{\partial h}$	$c=\frac{K_s}{\left(\theta_s-\theta_r\right)}\Theta^{m-1}$	$c=\frac{u}{\theta_e}$	$c=\frac{u}{S_S}$

Notation of Table: m is a parameter for power law equation; the average pore velocity v (LT^{-1}); θ_r (-) is the residual water content of the specific water capacity, θ_s (-) is the water content under saturation state, K_s (LT^{-1}) is the saturated hydraulic conductivity, and S_S (L^{-1}) is the specific storage.

3.4 Evapotranspiration and its modelling approaches

Climate change may cause variations on metrological forcing of precipitation, temperature, radiation, humidity, and wind speed, while, ecosystem change or human activity may affect the LAI, stomata behaviours, albedo, surface roughness, and soil hydraulic properties. All changing variables in the system are interacted and related with the evapotranspiration processes.

Evapotranspiration (ET) drives the hydrological process through energy-driven water-phase changes between systems of soil-vegetation-atmosphere, which performs a rather complex process attributable to the spatial and temporal variation (Gharun et al. 2014: Eagleson, 1982; Rodriguez-Iturbe and Porporato, 2004). ET is one of the components in water balance which is usually quantified by indirect estimation approach of combining measurement and modelling approach in the open environmental system. For instance, for large-scaled estimation, one can use an empirical function of air temperature and precipitation. For this type of study, identifying the components of ET is vital for understanding how ET is regulated is crucial for water yield management in water supply catchments.

In a vegetated area, ET consists of three components: interception, transpiration, and soil evaporation (Savenije, 2004; Lawrence *et al.*, 2007; Blyth and Harding, 2011), and its rate is affected by meteorological condition, vegetation dynamics, and also strongly interacted with the soil moisture and temperature dynamics of the near-surface soil profile (Entekhabi *et al.*, 1996; Rodriguez-Iturbe, 2000; Seneviratne *et al.*, 2010). Specifically, the interception diminishes the precipitation (both amount and intensity) that arrives at soil surface causing more gradual infiltration, and the infiltrated precipitation can increase soil moisture that will be subsequently consumed for transpiration and soil evaporation. Transpiration is directly conducted through the opening stomata of leaves to obtain carbon for photosynthesis, and simultaneously consumes soil moisture in the root zone by uptake process. The transpiration rates is governed by the physiological behaviour of leaf stomata, which is dictated by the meteorological conditions and soil moisture stress (Rao and Agaewal, 1984; Lin *et al.*, 2015). Moreover, the distinct canopy characteristics (e.g., leaf area and leaf morphology) (Vertessy *et al.*, 1995; Granier *et al.*, 2000; Roberts, 2000) and stand characteristics (e.g. stand age and structure) (Vertessy *et al.*, 1995; Ewers *et al.*, 2005) also affect the pattern of transpiration. As a result, actual rates of ET are less than potential rates due to the variable resistance of leaves to molecular diffusion of water to the atmosphere, imposed by stomata and other features of plant leaves (Dickinson et al., 1991). Soil evaporation delivers water from unsaturated zone to soil surface, which is sustained by moisture transport driven by liquid water exfiltration, phase change, and upward vapour flow. Additionally, the moisture and temperature dynamics on soil surface mutually dictate the variations of albedo, emissivity, and vapour pressure, which influence the energy budget and evaporation fluxes (Eltahir, 1998; Seneviratne *et al.*, 2010).

Understanding evaporation interaction with land and climate is essential, because ET holds a key role in regulating hydrological flows as well as atmospheric feedback. Consequently, quantification of the land-atmosphere interaction needs an integrated modelling system that incorporates theories from soil physics, vegetation physiology, and atmospheric science (Gran *et al.*, 2011). Such an integrated model provides a vertical "view" of the energy and mass transfers in a soil–vegetation–atmosphere transfer (SVAT) continuum. The details of SVAT model scheme were further described in **Chapter 5.4.3**.

In snow-dominated mountain environments, understanding how vegetation water use will change with warming requires taking a coupled eco-hydrologic perspective. There is a need to understand the interactions between vegetation characteristics and changes in the hydrologic cycle, including reduced and earlier snowmelt, changes in precipitation, as well as interactions among radiation, temperature, and vapour pressure deficits as drivers of ET. Therefore, understanding the stomatal conductance of certain tree species is vital to evaluation of local or region ET rate.

For estimating the evapotranspiration fluxes, many methods have been used a combination of physical principles with local-scale measurements, such as lysimeter, eddy covariance, and sap flow measurement. Those evapotranspiration measurements estimate either the total amount (e.g. Eddy covariance and lysimeter) or transpiration (e.g. sap flow) alone, however, all of which need expensive equipment, systematic calibration and regular maintenance (Zhou et al. 2006, Abraha and Savage 2012, Allen et al. 2011). Therefore, an advanced physical-based model combined with the long-term hydrometeorological measurements data is necessary to be developed, calibrated, and validated for supporting the hydrological simulation and prediction under a long time span.

The current physical-based hydrological model focuses on describing the water cycle in a hillslope/catchment, yet the energy cycle is not sufficiently addressed, which often estimates the potential evapotranspiration (i.e. the quantity of evapotranspiration when sufficient water is available) with a standard Penman-Monteith equation (Allen *et al.*, 1998) or a Shuttleworth-Wallace equation (Zhou *et al.*, 2006; Ridler *et al.*, 2014), though, the actual evapotranspiration is commonly calibrated by assuming the catchment is a closed system in which controls water storage and evapotranspiration with water inputs (e.g. precipitation) and outputs (e.g. streamflow and groundwater leakage). To sum-up, water-balance-based methods highly rely on long-term measurements of precipitation and stream discharge, still, the energy balance is far not rigorously satisfying.

Land-surface models here are developed to integrate water, vapour, momentum, and carbon fluxes to support the climate prediction at a global scale. Such model adopts a detailed leaf physiological measurement of stomatal behaviour to study the feedback mechanism of vegetation characteristics with respect to canopy structure, leaf area index (LAI), and stomatal conductance under the changing environment. The benchmark studies among land-surface models indicate that the simplification of soil physical and hydrological module may result in a difference (maybe physically unrealistic) in the soil moisture distribution, and weaken the simulating ability on the energy fluxes.

4. CASE STUDIES OF THESIS

The above-risen research questions were examined in various environments, enabling to study the effects of climate change and LULC change on the hydrological processes in different spatial and temporal scales. The results were demonstrated on the following case studies in 7 papers (where the stars marks indicate working as the corresponding author), representing the core of the research agenda within the doctoral studies.

Paper I. Langhammer, J., Su, Y., and Kaiglová, J., 2015. Runoff Response to Climate Warming and Forest Disturbance in a Mid-Mountain Basin. *Water*, 7, 3320-3342. DOI:10.3390/w7073320

The research area located in a Mid-Mountain Basin (upper Vydra basin), experiencing both climate change and bark beetle induced forest disturbance. Such a case offered a unique opportunity to examine the complexity of the accumulative impact of climate change and land cover change on runoff regime. Based on long-term hydro-climatic data, this study using a combination of statistical analyses to show existing changes in different runoff regimes. The observed changes in the mid-mountain basin highlight the sensitivity of such a hydrological system. The complexity with the changing environment also poses the importance of follow-up researches in this field.

Paper II. Jarsjo, J., Törnqvist, R., and Su, Y., 2017. Climate-driven change of nitrogen retention–attenuation near irrigated fields: multi-model projections for Central Asia. *Environmental Earth Sciences*, 76, 117. DOI:10.1007/s12665-017-6418-y

The research area located in the semi-arid region with intensive irrigation practices, high water losses through ET and increased concentration of nutrients and pesticides under climate change were challenging the regional ecohydrological system. The existing studies in this region drove research focus to model the potential hydrological responses under different climate change scenarios. The hydrological simulations assisted to further calculate the changes of nitrogen concentration under the projected climate-related runoff change. The climate-driven changes of hydro-chemical conditions are likely to be shared with many highly managed basins in arid and semiarid regions worldwide.

Paper III. Su Y., Langhammer, J., and Jarsjo, J., 2017. Geochemical responses of forested catchments to bark beetle infestation: Evidence from high frequency in-stream electrical conductivity monitoring. *Journal of Hydrology*, 550, 635-649. DOI:10.1016/j.jhydrol.2017.05.035

In the bark beetle-infested upper Vydra basin, four nested small catchments were selected as the study sites to investigate the hydrological and geochemical responses at different stages after the insect-induced forest disturbance. The high frequency and long term monitoring of in-stream electrical conductivity (EC), hydro-climatic conditions, and vegetation dynamics allowed using EC as indicators to conduct hypotheses for possible runoff generation mechanisms and understand the potential geochemical transformation processes. The comparisons between catchments and within each catchment provided solid signals of the changes in hydrogeochemical conditions. Considering the current observations, projections of continued climate warming, and the increasing spread of bark beetle outbreaks in the mid-latitudes, understand the insect-induced hydrogeochemical changes at the catchment-scale is vital for forested regions worldwide.

Paper IV. Shao, W., Su, Y.*, Yang Z., Ma, X., and Langhammer, J., 2018. Quantify the pore water velocity distribution by a celerity function. *Geofluids*, 2018, 19. DOI:10.1155/2018/1054730.

Under the study of using EC as a tracer to understand the runoff generation process, the difference of celerity-velocity opened a new direction to better understand the water flow and tracer transport in the subsurface system. This study attempted to investigate the mechanism of pressure propagation and tracer transport in a subsurface flow system by analysing the celerity in unsaturated flow. This initial attempt was at a theoretical basis, a celerity function was proposed based on a pore bundle model and explained how to use it for potential subsurface flow analysis. Commonly used breakthrough curves can be derived from the proposed celerity function, which offers a possibility to quantify the advective tracer transport for different soils.

Paper V. Shao, W., Su, Y., and Langhammer, J., 2017. Simulations of coupled non-isothermal soil moisture transport and evaporation fluxes in a forest area. *Journal of hydrology and hydromechanics*, 66, 1-6. DOI: 10.1515/johh-2017-0038

Paper VI. Shao, W., Coenders-Gerrits, M., Judge, J., Zeng, Y., Su, Y.*, 2018. Simulation of non-isothermal soil moisture transport and evaporation fluxes in a maize cropland. *Journal of Hydrology*, 561, 833-847. DOI: 10.1016/j.jhydrol.2018.04.033.

Two studies were carried on to show great potential to incorporate well-established land-surface scheme and parameterization strategies with a physical-based subsurface hydrological model to build a new soil-vegetation-atmosphere transport (SVAT) model. Such a process-based model, based on physical principles and current scientific understanding of relevant processes of soil physics, hydrological and meteorological science, results in a more reliable and accurate prediction of evapotranspiration and streamflow under the changing environment. We tested the model in the forested area over the vegetation period (summer) as well as in designed crop plot with changing LAI to show the performance. Two study areas had intensive measurements of water and energy fluxes, which allowed to validate the model being prepared for the region with limited water and energy measurements but only simple climatic data.

Paper VII. Su, Y. *, Shao, W., Vlcek, L. and Langhammer, J., 2019. Ecohydrological Behaviour of Mountain Beech Forest: Quantification of Stomatal Conductance Using Sap Flow Measurements. Geosciences, 9(5), 243. DOI: 10.3390/geosciences9050243.

Stemming from the interests in ET, transpiration is one of the key components of the evaporation fluxes in forested area. Therefore, accurate estimation of the ET largely depends on how to calculate the transpiration, in particular in a basin has changed significantly in its forest status. An experimental plot was set up in the upper Vydra basin, the sap flow of beech trees was measured with high-frequency from vegetative to deciduous period for investigating transpiration pattern. The stomatal conductance was reversely calculated based on the parametrization of Jarvis-Stewart model, which can also help to better understanding the evapotranspiration process in newly formed beech stands after bark beetle outbreak in central Europe.

5. STUDY AREAS, MATERIALS AND METHODS

5.1 Study areas

Two main research areas were selected aiming to examine the ecohydrological conditions at varying spatial and temporal scales. One basin, the ASDB, undergone anthropogenic disturbance with large-scale irrigation intensification in a semi-arid region of Central Asia, and this study area was used for **Paper II**. Another basin, the upper Vydra basin, undergone natural disturbance with bark beetle infestation in a mid-mountain region of Central Europe, and this study area was used for **Paper I, III, and VII**. Such two terrestrial basins where have diverting environmental problems were used for this thesis together to understand the ecohydrological processes and dynamics under different environment.

Aral Sea Drainage Basin, Central Asia

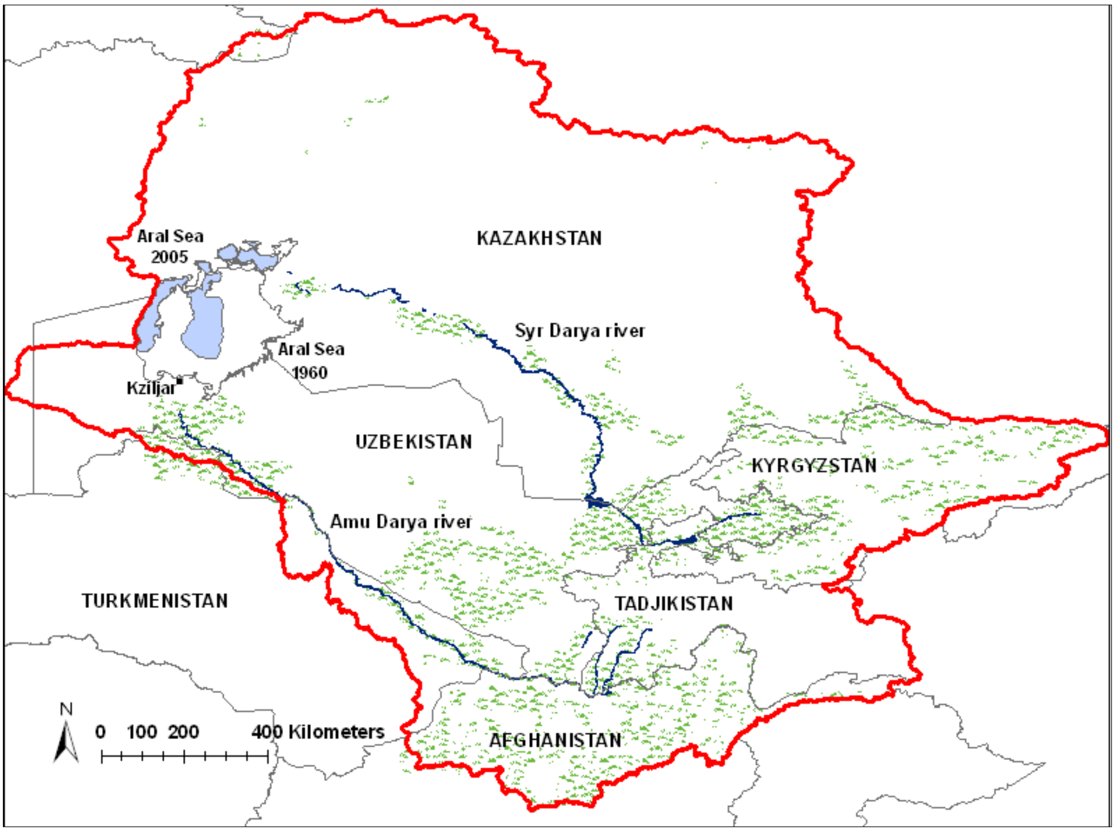

***Figure 3**. Location map of the Aral Sea Drainage Basin, Central Asia, and its two principal rivers Amu Darya and Syr Darya. Irrigated areas are shown in green. The size of Aral Sea is given for the year of 1960 and 2005.*

The ASDB given in Fig. 3 owns an area of 1 874 000 km^2, covering the main part of Central Asia, which is shared by six countries - Kazakhstan, Turkmenistan, Uzbekistan, Afghanistan, Kyrgyzstan, and Tajikistan. Two principal rivers - Amu Darya and Syr Darya - originate in the mountains of Tajikistan and Kyrgyzstan, which are the sources of 67% of ASDB's renewable water resources from. The Amu Darya River Basin (ADRB) has an extent of 465 000 km^2 (Asarin et al., 2010). The endorheic ASDB has an arid continental and semi-arid climate with extreme temporal and spatial variation of precipitation and temperature owning to its broadly variable topographical, geological and geographical structures (Lioubimtseva and Henebry, 2009).

The agriculture in ASDB largely relies on a surface irrigation system, and the extent of the irrigated areas increased rapidly from 2.5 million hectares (ha) in 1910 to 7.4 million ha (i.e. occupy 75% of the area) in 1990 (Jarsjö *et al.*, 2011). More than 90% of the total river runoff in the downstream regions is currently diverted through irrigation canals to irrigated fields (Cai et al., 2003). The river runoff was decreased from 70 km^3 year^{-1} before irrigation started down to around 6 m^3 s^{-1}h after1980. The agriculture there generally has a high utilization rate of fertilizer and pesticide, which contains high N (Törnqvist *et al.*, 2011). Consequently, after the irrigation started the total amount of N applied to the basin was increased from 160 000 ton year^{-1} in 1960 up to 420 000 ton year^{-1} in 2000 (Jarsjö *et al.*, 2017).

Upper Vydra Basin, Central Europe

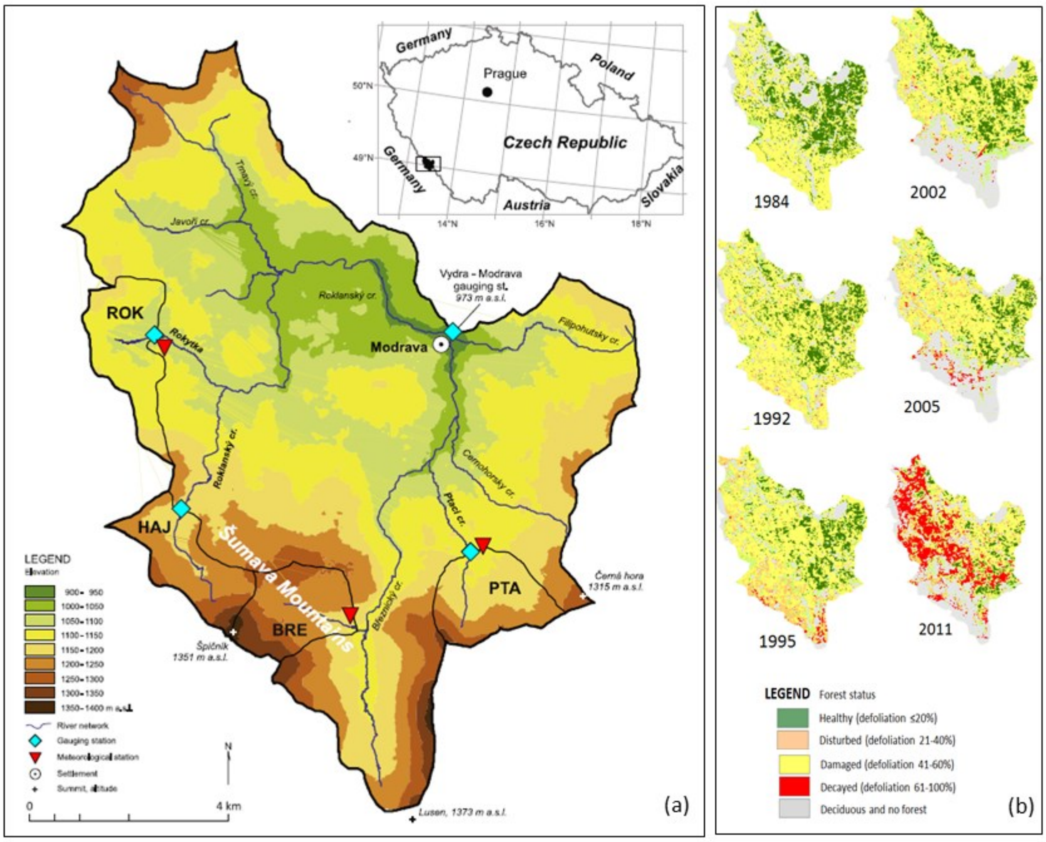

Figure 4. a) *The location of the upper Vydra basin, ending at the Modrava gauging station (49° 1' 30.0216" N, 13° 29' 47.1624" E). The location and border of four experimental catchments are given with names.* ***b)*** *Forest cover change as a result of bark beetle infestation over the year 1984-2011.*

The upper Vydra basin covering 90.1 km^2 is located in Sumava National park, in Central Europe (Fig. 4a). This region has typical mid-latitude montane climate featuring with 3.6 ºC of mean annual air temperature and 1 370 of mean annual precipitation, from which approximately 40 % comes as snow (Kliment *et al.*, 2011; Langhammer *et al.*, 2015). As it is the headwater area, the area consists of many small streams, and the hydrological responses to rainfall events are relatively fast. The annual discharge rate is 3.34 $m^3\ s^{-1}$.

Since the 1990s, one of the dominant tree species - Norway spruce (*Picea abies*) - has started to be subject to bark beetle (Ips typographus [L.]) infestations, which caused more than 50% of the basin experienced tree mortality in 2010 and some areas have regenerated relatively rapidly now (Hais *et al.*, 2009; Langhammer *et al.*, 2015) (see Fig. 4b).

5.2 Field experiments

Nested experimental catchments

Table 2. *Basic physiographic and land cover characteristics of the four experimental catchments. The red dots in the maps indicate the locations taken water samples for snapshot analysis.*

Catchment	PTA	ROK	HAJ	BRE	Legend & unit
Topography & snapshot locations	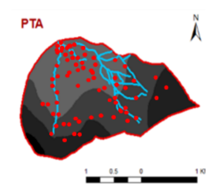	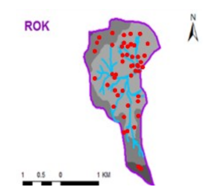	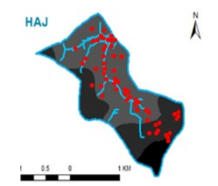	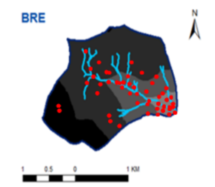	River network DEM [m a.s.l.] 970 - 1019 1020 - 1079 1080 - 1129 1130 - 1179 1180 - 1229 1230 - 1299 1300 - 1379
Vegetation dynamics	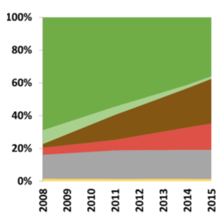	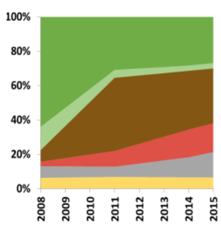	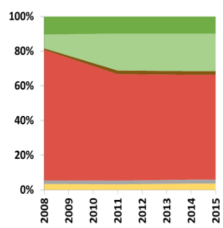	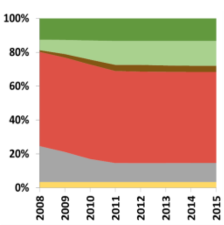	Healthy forest Regenerated forest Damaged forest Decayed forest Non-forest Meadows
Initial year of major infestation	2014 (least disturbed)	2010 (newly disturbed)	< 1996* (highly disturbed)	<1996* (highly disturbed)	

*Note: * the initial year of major bark beetle infestation in HAJ and BRE was between 1984-1995 (Hais et al., 2009; Langhammer et al., 2015).*

The hydro-meteorological monitoring is based on the automated sensor network consisting of 11 gauging stations successively installed in the study area by Charles University in Prague (CUNI) since 2005.

Among these potential study areas, four experimental catchments - Hajenka (HAJ), Breznicky (BRE), Rokytka (ROK), and Ptaci (PTA) - were established (Fig. 4a) to study the ecohydrological behaviours in a higher spatial resolution with more intensive temporal resolution. Four catchments represent different stages and magnitudes of bark beetle-induced forest disturbance, ranging from essentially healthy to heavily damaged catchment over the monitoring period (see Table 2).

In these four experimental catchments, hydrological stations (see Fig. 4a) measured water table and EC at 10-minute intervals from 2009 till now. The water stages were converted to streamflow (Q in m^3 s^{-1}) using the rating curve, which was derived by hydrometric measurements using an acoustic Doppler velocimeter and a salt dilution method (Su and Langhammer, 2014). Water samples of precipitation were collected from Modravsky meteorological station since 2013, which assisted in obtaining the characteristics of long-term precipitation EC.

For each site, snapshot sampling methods were used to obtain EC in different locations and at multiple vertical layers including surface water, spring water, soil water, and groundwater, and Table 2 showed the snapshot sampling locations.

Sap flow experimental plot

In the ROK catchment, we selected two locations, K1 and K2, installing two tensiometers (T8 Tensiometer, UMS) to measure soil pore water pressure and soil temperature at depth of 20 cm and 60 cm in the soil with 30-min interval (Fig. 5ab). The probe K1 is located in former spruce forest (Picea abies), now is covered with dead spruce forest stands caused by bark beetle outbreak, and small seedlings, and a new generation of spruce forest. We used this study area for applying the SVAT model.

At the K2 location, six beech trees with different ages and truck diameters were installed with EMS 81 sap flow sensor (EMS Brno, CZ) within a square area (30×30 m) of 900 m² in this study (Fig. 5cd). The square area consisted of 32 beech trees with the mean age of 55 years and the mean trunk diameter of 0.9 m (at a height of 1 m) (Fig.5e). The leaf area index (LAI) was measured by hemispherical photos. The photos were taken by camera Nikon COOLPIX 995 with Nikon Fisheye lens Converter FC - E8 0.21x in a square (30x30 m) in a step of 10 m. Thus, 16 pictures were taken and analyzed for leaf area index in Gap Light Analyzer (GLA) software (Frazer et al., 1999).

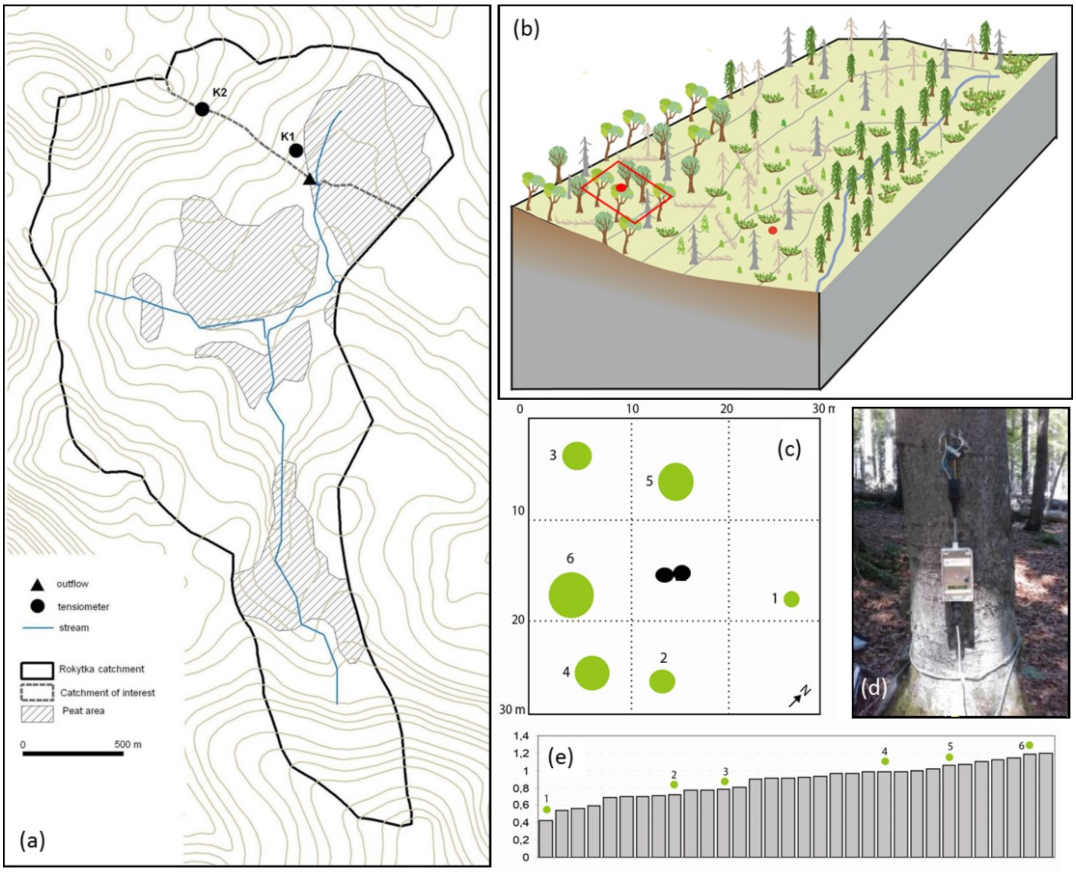

***Figure 5. (a-b)** Study area –ROK and the location of the plot. **(c)** Scheme of tree distribution for sap flow measurement at the 30x30 m experimental plot. The size of the green dot represents the size of the tree trunk. **d)** Photo of one installed EMS 81 sap flow device at 1 m above the ground in Tree No. 1. **e)** Tree trunk diameter (unit in m) distribution at 1m height within 32 beech trees over the experimental plot. Note: the green dots mark the measured trees.*

5.3 Data synthesis and analysis

For a long-term historical study for the upper Vydra basin (**Paper I**), daily and monthly hydro-climatic long-term observations (1961–2010) of precipitation, air temperature, and discharge were obtained from the various Czech Hydrometeorological Institution (CHMI) stations. Based on the data, statistical and analytical methods were applied including double-mass curve analysis, recursive digital filter, Mann-Kendall test, CUSUM analysis, Buishand's and Petitt´s homogeneity tests, and ordinary Kriging.

In the upper Vydra basin, four nested catchments (**Paper III**) were selected and using high frequent hydro-climatic data together with EC to study the responses of hydro-geochemical behavior in each catchment under different forest disturbance stages. The hydrochemistry for the pre-infestation comprising in total of 115 measurements in the study area resulted from Vesely and Majer, (1998)'s study in the 1990s and Ruzicková and Kotrbová (2000)'s study during 1997. The data were aggregated in yearly, daily and hourly values according to the temporal resolutions required by the different analytical methods applied including Mann-Kendall test, Pearson correlation test, Friedman test, etc. At the event-scale analysis, method proposed by Zuecco et al. (2016) was used to categorize the EC-Q hysteresis loop (see **Chapter 5.4.2**).

The modelling approach was used in **Paper II** to study the impact of climate change on future streamflow and nitrogen concentration. Outputs of changed T and P from 73 GCM projections (∆T and ∆P) for different time periods following the reference period 1961-1990 were extracted from two previous studies (Jarsjö et al., 2012; Lioubimtseva and Henebry, 2009). The results were used as input in the hydrological modelling and further calculated in the nitrogen retention-attenuation model (**Chapter 5.4.1**).

In the theoretical analysis in **Paper IV**, the celerity was firstly defined according to the continuum equations, and then based on the conceptualization of a pore bundle model, a mathematical derivation and the kinematic ratio can be illustrated. Under unit hydraulic gradient condition, the celerity function is formulated as a first-order derivative of the soil hydraulic conductivity function to manifest the pore water velocity distribution, which can further be used to derive a breakthrough curve. The soil hydraulic characteristic of typical soil textures is re-analysed by using the unmodified and modified Mualem-van Genuchten and Brooks-Corey models with standard parameter sets. In the end, the celerity-effective saturation curve was applicable to the bimodal soil hydraulic functions to demonstrate the distributions of pore water velocities for natural soil.

Newly proposed SVAT model (**Chapter 5.4.3**) only required the measurements of net radiation, rainfall, atmospheric temperature, wind speed, and air humidity as the model input. Two study sites (**Paper V, VI**) were used for testing the performance of the model, and the model performance is evaluated by comparing simulations with measurements using the bias and root-mean square error (RMSE), including the energy fluxes of latent heat, sensible heat, and ground heat fluxes, as well as soil temperature and soil moisture content at different soil depths. The sap flow technique was used to obtain transpiration rate (see **Chapter 5.2**), which was used to infer the stomatal conductance (see **Chapter 5.4.4**). In **Paper VII**, the Jarvis-Stewart model was used to describe the response of stomatal conductance under the multiple environmental stress of net radiation (Rs), vapour pressure deficit (D), temperature (T), and soil moisture content (θ). Moreover, the impact of parametrization of stomatal conductance on transpiration rate was quantified with two methods: one used inversely estimated stomatal conductance, and the other used typical stomatal conductance of broad leaf forest adopted from a lookup table in an existing literature. Finally, the pattern of transpiration rate during the transition period from vegetative period to defoliated period was analysed.

5.4 Quantification methodologies

5.4.1 Semi-distributed hydrological model and nitrogen retention-attenuation model

The water flow routines of the PCRaster based Polflow model (De Wit 2001) were used to quantify the changes in river discharge from projected future climate change(Shibuo et al. 2007; Destouni et al. 2010; Jarsjö et al. 2012; Törnqvist and Jarsjö 2012; Asokan et al. 2010). The model is based on a water balance approach of Q=P-ET-ΔS, where ΔS is the storage change which is assumed to be negligible on the considered long-term basis. Under current irrigation practices, the modelling in this study described in Shibuo et al. (2007) and Jarsjö et al. (2012) to examine climate change impacts. P and T data from CRU TS 2.1 database (Mitchell and Jones, 2005) was used to calculate potential ET (ETp) using Langbein method (1949) and actual ET (ETa) using Turc method (Turc 1954). Irrigation water was rerouted from the river to irrigated areas according to Global map of irrigated areas (Siebert et al., 2005) and applied as extra precipitation. Digital elevation data from Shuttle Radar Topography Mission (SRTM 2004), was used to generate flow pathways and flow accumulation of runoff R expressed as R=P-ETa. The river discharge (Q) in a specific point was generated as the sum of flow accumulation in all contributing upstream grid cells.

We used the paired △T and △P output from the considered 73 GCM models mentioned in **Chapter 5.3**, the hydrological model would be run 73 times. We here instead discretize the total prediction envelopes of △T and △P using even spacing, choosing a resolution that gives a matrix of 11*11 nodes that hence requires a total of 121 runs of the hydrological model. The △T and △P values of each node are then added to an observed historical baseline map (from the CRU TS 2.1 database; Mitchell and Jones, 2005) of current temperature (T_0) and current precipitation (P_0), i.e., $T_{(modelled)} = T_0 + \Delta T_i$ and $P_{(modelled)} = P_0 + \Delta P_j$. This results in 121 maps with distributed runoff values, from which the cumulative river discharge $Q_{(modelled)}$ at the basin outlet are extracted (more hydrological model details are given in a separate paragraph below). The 121 values of $Q_{(modelled)}$ hence correspond to the 121 different combinations of T_0+△T and P_0+△P according to the nodes of the matrix. The change in river discharge $\Delta Q_{(modelled)}$ is obtained by subtracting a $Q_{0\ (modelled)}$ result from $Q_{(modelled)}$, where $Q_{0\ (modelled)}$ is obtained for △T=0 and △Q=0. The values of those nodes are finally interpolated to produce a continuous hydrological response map that visualizes the responses of river flow to climate change.

Analogous to the work of Törnqvist et al. (2015) we assume that nitrogen undergoes first-order degradation along hydrological flow-pathways, expressed as exp[-λT], where λ is the attenuation rate and T is the mean travel time. The magnitude of internal flow redistribution within the basin is characterized by a water recirculation ratio r, as defined previously in Fig.1b. A certain fraction (f) of Q_{div} is assumed to be lost through ET over the irrigated fields. This dimensionless fraction is expressed as $f = ET_{irr}/Q_{div}$ where ET_{irr} is the additional ET (expressed in units of flow) from the irrigation of the basin. ET_{irr} was calculated from the hydrological modelling as the total ET under conditions of irrigation and water rerouting ($ET_{irr+nat}$) minus natural ET_{nat}, i.e., ET without rerouting of river water. The nitrogen attenuation rate λ was further assumed to change as function of r due to increased flow-path lengths, where λ(r) = λ(1 + αr) and α is a constant that allows for the different significance of r on the attenuation effect for different conditions. The outflow-inflow concentration ratio (C_{out}/C_{in}) can then be expressed analytically as (Törnqvist et al. 2015):

$$C_{out}(r)/C_{in} = \frac{1+fr}{1+r}\exp[\beta \cdot \lambda T] \Big/ \left(1 - \frac{r}{r+1}\exp[\beta \cdot \lambda T]\right) \quad (1)$$

where $\beta = (1 + \alpha r)\cdot((f \; 1)r/(1 + fr) \;\; 1)^{1}$, $C_{out}(r)$ is the concentration at the basin outlet, and C_{in} is the concentration of upstream runoff.

An effective value of the basin-scale attenuation product λT for nitrogen was estimated by matching Equation (1) to observation data from the 20-year period 1960-1980 with a low r-value (1.4). The basin characteristic λT-value was then tested to fit observation data from 1981-2000 that were characterized by a much larger r (5.7) due to irrigation intensification. For these periods, monthly observations of dissolved inorganic nitrogen concentrations [DIN] were available from at Kziljar gauging station close to the Aral Sea outlet (Nasrulin and Zahidova 2002). Dissolved inorganic nitrogen concentrations were computed as the sum of NO_3-N, NO_2-N, and NH_4-N concentrations. As also explained in Törnqvist et al. (2015), the main reason for focusing on DIN is that it comprises highly soluble and dominant (in particular NO_3^-) forms of nitrogen in agriculturally impacted river systems, and since monitoring data existed for these fractions. The data was used to estimate C_{out} (r=1.4) and C_{out}(r=5.7). Corresponding C_{in} values were calculated as basin-scale N input not taken up by crops divided by upstream modelled R ($R=P-ET_{nat}$). The derived basin-scale value of λT for nitrogen was used in combination with GCM-based projections of future river flow to estimate possible climate-driven changes in riverine nitrogen concentrations at the outlet.

5.4.2 Tracer hysteresis evaluation model

In the event-scale analysis, refined hourly data were used. Specifically, an event is defined as the periods with more than 0.2mm/h of rainfall (Muñoz-Villers and McDonnell, 2013), and separated by a dry period of at least 6h (Sidle et al., 2000). Furthermore, the standard deviation of precipitation (P_{SD}, -), mean intensity (PI, mm/h) and maximum intensity (PI_{max}, mm/h) of each rainfall event is calculated based on data from at least 5 stations to ensure the runoff behavior of each catchment in response to relatively similar rainfall conditions. The indices of total runoff depth (R, mm), RC (i.e., R/P), lag time between rainfall peak and discharge peak ($T_{lag(P\text{-}Q)}$, h), lag time between EC peak and discharge peak ($T_{lag\,(EC\text{-}Q)}$, h), coefficient of determination between EC and R (r^2,-), the duration of the rising limb (T_r, h), and maximum EC (EC_{max}, μs/cm) was calculated.

We employed the method proposed by Zuecco et al. (2016) to categorize the EC-Q hysteresis loop based on its direction, shape, and size. First, Q and EC data were normalized to range between 0 and 1 as Q′(-) and EC′(-) (Su *et al.*, 2017). Based on Zuecco et al. (2016), the difference $\Delta A_{[i,j]}$ in the definite integrals of the rising and falling parts of the hysteresis curves was calculated as follows:

$$\Delta A_{[i,j]} = \Delta A_{r[i,j]} - \Delta A_{f[i,j]} = \int_i^j EC'r(Q')dQ' - \int_i^j EC'f(Q')dQ' \quad (2)$$

In this study, we set the intervals of integrations as 0.05 using a linear function, with an equal width between the lower and upper limits of integration. Values of minimum, maximum, and the sum of $\Delta A_{[i,j]}$ were calculated and used as the indices, denoted as ΔA_{min}, ΔA_{max}, and ΔA_{sum}, respectively. Following the procedure given by Zuecco et al. (2016), these indices were then used to determine one of eight identified EC-Q hysteresis classes. If the dependent variable decreases from the initial state, eight types can be identified.

5.4.3 SVAT Model

The model proposed in **Paper V** and **Paper VI** conceptualized the energy and water transport (Fig. 6). The land-surface module in Fig.6a describes the energy and vapour transport soil-canopy evapotranspiration system. Radiative transfer is quantity the incoming and outgoing long-wave and short-wave radiation fluxes separately, and estimate net radiation energy of the canopy layer and soil surface layer. A two-layer energy network is designed to facility the partitioning of the evapotranspiration into transpiration, soil evaporation and interception evaporation, which driven by the energy fluxes component of latent heat, sensible heat and ground heat fluxes and connected with resistance coefficients. The influence of radiation, foliage temperature, vapour pressure deficit and soil moisture deficit on stomatal resistance and transpiration will be explicitly formulated by the Jarvis-Stewart (JS) model to introducing the dynamic interaction between transpiration and environmental stress (Jarvis 1976, Stewart 1988) (This JS model was further used in **Paper VII** when calculating the stomatal conductance, see **Chapter 5.4.4**). The influence of soil moisture deficit on evaporation reduction is formulated with soil surface resistance equation (van de Griend and Owe 1994). The aerodynamic resistance coefficients are formulated by widely-used Monin-Obukhow similarity theory and eddy diffusion theories to support the land-surface-atmosphere interaction (Choudhury and Monteith 1988, Sellers et al. 1996).

The canopy hydrology in Fig 6b describes the processes of the interception and throughfall, and the E_t and E_i. Rainfall Initially reaches the vegetation canopy, some of which can penetrate through the canopy directly reaching the soil surface, while, some of which will be intercepted by the leaves and branches of vegetation canopy, and along with the canopy interception storage increasing, throughfall, and stem flow (summed as water dripping) will be formed. Canopy hydrology process is calculated by a water balance equation (Eltahir and Bras 1993). The total water uptake by plant is equal to the actual transpiration rate, but spatially distributed water uptake is according to the variation of soil moisture and root density distribution. In the water scarce region, the diminished water uptake rate of upper and dryer soil layers are compensated by the enhanced water uptake form the lower wetter layers (Yadav et al. 2009).

The soil multi-phase flow in Fig 6c describes the water, vapour, air, and heat transport in a root zone to more accurately describe the energy balance in the subsurface system. The liquid water flow is described by the equation of Darcy-Richards, the upper boundary conditions include flux boundary condition for non-ponding infiltration and the pressure head boundary when ponding and overland flow occurs. The vapour flow (gas phase) is a convection-diffusion equation with the upper boundary of soil evaporation rate, and the airflow is simplifying considered to enhance evaporation during the drought condition. The heat flow equation includes thermal convection (originated from the mass transport of water, air, and vapor flow), and thermal conduction. The group of equations is coupled with the source/sink term of vaporization/condensation and root water uptake treated as a fully coupled PDEs system, and simultaneously solved by finite difference numerical approaches (Celia et al. 1990, Pinder and Celia 2006) and combined with the Picard iteration technique (Grifoll et al. 2005).

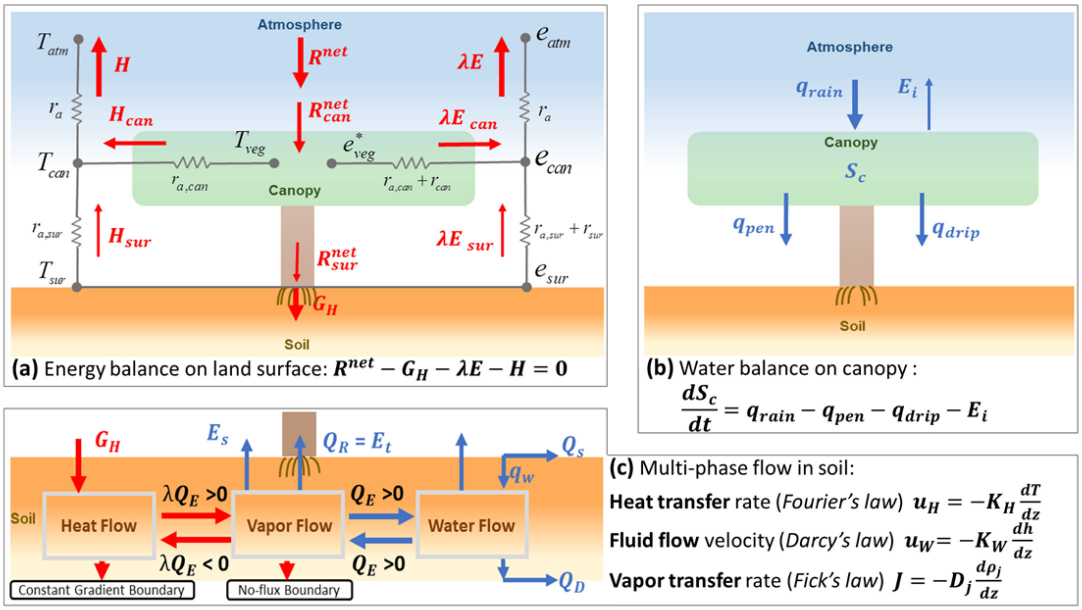

Figure 6. *SVAT Model conceptualization and governing equations/theories of each module.* E_t, E_S, *and* E_i *is transpiration, soil evaporation, and canopy interception evaporation. All red arrows represent the energy flux and the blue arrows indicate water flux. Air temperature, precipitation, wind, and humidity are the input for the model. The detailed components and used coupling approaches.*

5.4.4 Stomatal conductance model

The potential evapotranspiration (i.e. the amount of water evaporates to the atmosphere with a sufficient water supply) from a single-layer system can be estimated by the latent heat flux density through the analytically-expressed PM equation, which was done in **Paper VII**. In the vegetated area, transpiration rate is dictated by the parameter of stomatal conductance, g_c(m s^{-1}). If the transpiration rate (e.g., from sap flow measurement) and climatic measurements are available, the stomatal conductance then can be inversely estimated by rearranging the PM type equation:

$$g_c = \frac{g_a \gamma \lambda E}{\Delta R_{can} + \rho_a C_p (e_s - e_a) g_a - \lambda E(\Delta + \gamma)} \quad (3)$$

where E (mm s^{-1}) is the stand transpiration calculated from the sap flow measurements (Su *et al.*, 2019).

Generally, the stomatal conductance is controlled by the stomatal aperture in response to the availability of energy, carbon, and water in soil (Farquhar and Sharkey, 1982). Considering the impact of multiple environmental factors on stomatal conductance, this study adopted the JS model (Jarvis, 1976; Stewart, 1988) consists of multiplicative nonlinear functions of environmental variables (Jarvis, 1976; Zhang *et al.*, 2011; Naithani *et al.*, 2012; Wang *et al.*, 2014):

$$g_c = I_{LAI} g_{c,max} \prod_i F_i(x) \quad (4)$$

where I_{LAI} is the leaf area index (2.2 is the value used in this study), and $g_{c,max}$ (m s^{-1}) denotes the theoretical maximum g_c under the optimal water, nutrient, and climatic conditions.

The functions F_i are a set of scaling terms that reduced a maximum value of canopy conductance ($g_{c,max}$) in response to changes in net radiation (R_s), vapour pressure deficit (D), temperature (T), and soil water content (θ). The values of functions F_i range between 0 and 1, therefore any changes in the values of R_s, D, T, and θ will proportionally modify the parameters $g_{c,max}$ to give an estimations of g_c controlling transpiration rate. The following four multiplicative stress functions are taken from previous studies (Stewart, 1988; Magnani *et al.*, 1998; Granier *et al.*, 2000; Zhou *et al.*, 2006).

The response of transpiration to net radiation was presented by a hyperbolic saturating function at leaf, tree, and canopy scales (Stewart, 1988; Granier *et al.*, 2000; Zhou *et al.*, 2006).

$$F_1(R_s) = \frac{R_s}{1000}\frac{1000+k_c}{R_s+k_c} \quad (5)$$

where k_c is a fitted parameter describing the curvature.

The effect of vapour pressure deficit D(kPa) on canopy conductance is expressed by an exponential equation (Whitley *et al.*, 2009), which is traditionally defined by Jarvis (1976) and Stewart (1988):

$$F_2(D) = \exp(-kD) \quad (6)$$

where k is a free parameter, describing the decrease in g_c with increasing D.

The influence of temperature on canopy conductance was represented by a bell-shaped function (Jarvis, 1976; Magnani *et al.*, 1998; Zhang *et al.*, 2003)

$$F_3(T) = \frac{T-T_{min}}{T_{opt}-T_{min}}\left[\frac{T_{max}-T}{T_{max}-T_{opt}}\right]^{\frac{T_{max}-T_{opt}}{T_{opt}-T_{min}}} \quad (7)$$

where T_{min} and T_{max} (K) are minimum and maximum temperatures that indicate the temperatures below and above which complete stomatal closure occurs, and T_{opt} is the optimum temperature that indicates the temperature of maximum stomatal opening. Canopy temperature was assumed to equal air temperature, since temperature gradients are usually small in forest canopies (Magnani *et al.*, 1998).

The impact of soil water restrictions on canopy conductance is expressed by a three-phase relationship (Zhou *et al.*, 2006; Whitley *et al.*, 2009):

$$F_4(\theta) = \begin{cases} 1, & \theta \geq \theta_f \\ \frac{\theta - \theta_r}{\theta_f - \theta_r}, & \theta_r < \theta < \theta_f \\ 0, & \theta \leq \theta_r \end{cases} \tag{8}$$

where θ_f is the field capacity below which the plant transpires less than its maximum value, and θ_r is the residual soil moisture content, i.e., willing point below which the plant stops transpiration.

6. SYNTHESIS OF RESEARCH FINDINGS

6.1 Climate change and ecohydrological responses

In the study (**Paper I**) placed in the upper Vydra basin, Central Europe, the long term hydro-climatic changes over the period of 1961-2010 was analysed, and the results showed a clear increasing trend of annual air temperature, which was occurring in the rest of the world including another study area in Central Asia in **Paper II**. Under the climate warmer, the annual precipitation did now show consistent tendency in two places due to the heterogeneity of climate-land-vegetation-soil feedback. However, the apparent changes of the hydrological regimes were observed in both places, which all causing the changes in their geochemical conditions.

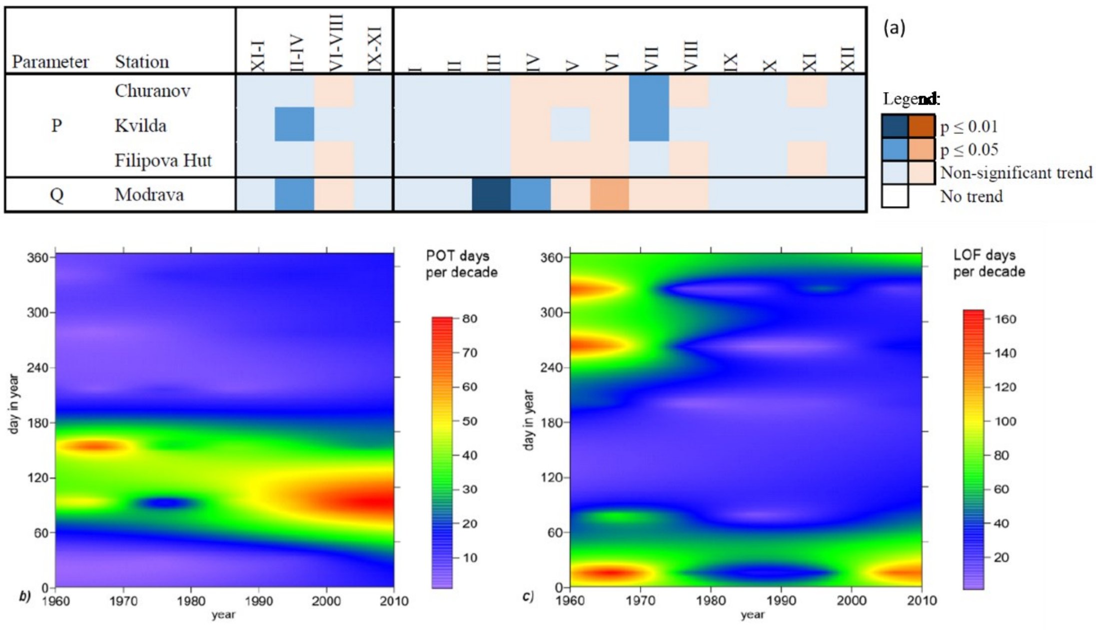

***Figure 7. (a)** Mann-Kendall test of seasonal and monthly trend of P and Q during 1961-2010. Blue indicates increasing trend while red indicates decreasing trend, and darker color indicates more significant trend. **(b)** Changes in frequency and seasonality of days with POT; and (**c**) Changes in frequency and seasonality of days with LOF.*

In the upper Vydra basin, forest disturbance was an add-in driving factor since the 1990s, and the observed changes mainly occurred in runoff seasonality and intra-annual variability but not the annual runoff balance. The seasonal runoff shifted from summers by an 18% decrease to springs by a 10% decrease (Fig.7, and more details see **Paper I**), which could largely attribute to the climate-driven changes in the snow-melting process. The occurrence of peak flows (POT) doubled but shifted from late spring to early spring (Fig. 7b), while the occurrence of low flow (LOF) shifted from autumn to mid-winter with a two-thirds decrease in days till 1990 followed an increase (Fig. 7c). Changes in POT and LOF may be caused by changes in forest cover due to bark beetle infestation. The observed runoff regime change indicates the sensitivity of the mid-latitude montane basin to climate change as well as to land cover change, and the inconsistency of the changes worldwide highlights the importance of more studies from the varying environment.

One important highlight from **Paper I** is the necessity of splitting the upper Vydra basin into smaller catchments to understand the impact of forest disturbance to the runoff regime before moving forward to project the future impact of climate change on the hydrological system.

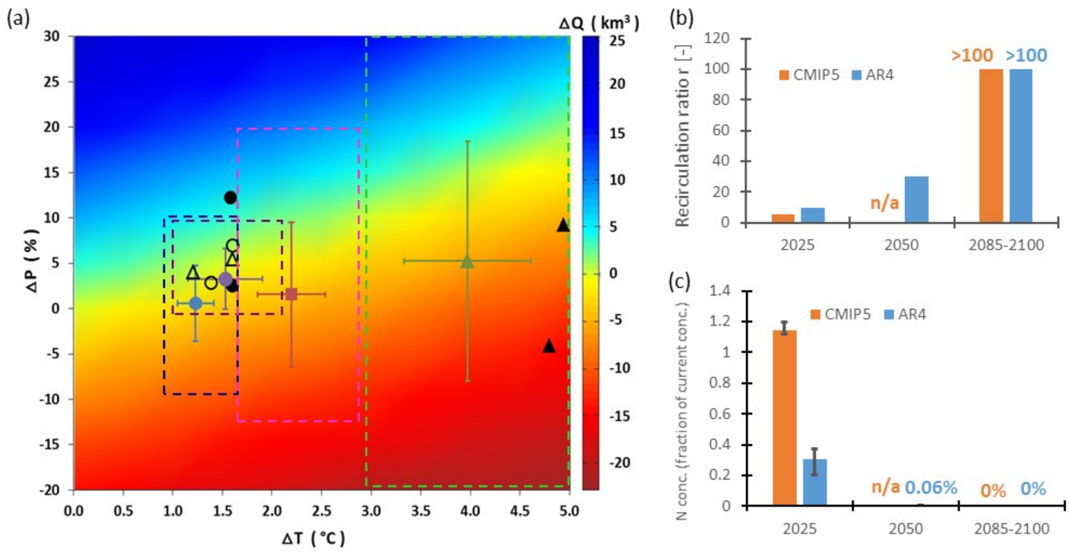

Figure 8. *(a) The modeled flow change ΔQ in the Amu Darya river near its outlet, in response to windows of ΔT and ΔP combinations that covers all ΔT and ΔP combinations of the considered 73 GCM projections including 14 GCM projections from AR4 for 2025 (Jarsjö et al. 2011), 51 GCM projections from AR4 for Central Asia around 2025, 2050 and 2100 (Lioubimtseva and Henebry 2009), and 8 output of the best-performing CMIP5 models for ASDB around 2025 and 2085 (Asokan et al., 2016) shown with black (triangles and square) symbols. The ensemble mean values and standard deviation of the multi-model output from AR4 are indicated with colored symbols and error bars;* ***(b)*** *r-value of ADRB and* ***(c)*** *N concentrations in its downstream river water in years 2025, 2050 and around 2085-2100, based on output from CMIP5 and AR4 climate models.*

Unlike the small basin, in the ASDB, when the spatial scale increased up to the large basin, the temporal scale was enhanced to annual mean conditions. The annual runoff decreased by around 70 km^3·year^1 during the 1960-2000, and the N fertilizer application in the ADRB and the water recirculation rate were increased. For the basin covering 1.3% of the earth's land with high population, the future climate-driven projections of changes in runoff regime and nitrogen retention-attenuation are crucial for the regional management and planning. **Paper II** found from converging 73 multi-model projections that ΔT= 5°C and ΔP=13 mm·year^1 in the region will likely cause ΔQ= - 7 km^3·year^1 (negative value indicates decrease comparing to the current condition) till 2100 in its principal Amu Darya River in 2100. As projected, once ΔQ= - 4 km^3·year^1, the degree of river water and irrigation water re-use (the recirculation ratio, r) will change from the current value of 5.7 to over 100 in 2100 under both scenarios (Fig. 8ab). Using a basin-scale analytical recirculation model adopted for nitrogen loading conditions of ADRB, the climate-driven enhancement of r-value may considerably decrease the riverine DIN-concentrations at the outlet (Fig. 8c). More generally, if current agricultural practices are maintained in ADRB, the recirculation of already saline return flows may increase in the future as the result of climate-related water shortage. The present results furthermore imply that such high sensitivity of riverine nitrogen concentrations to climate change can be common in highly managed basins across the world.

6.2 Geochemical response after bark beetle infestation

Table 3. *Summary of the findings in* ***Paper III****, listing the effects of insect-induced forest disturbance on in-stream EC at multiple timescales. The Fig. 9 summarized the EC characteristics in each studied catchment, which assisting in interpreting the findings.*

Multiple timescales	Findings in Paper III	Implications
Annual	• Increased annual average in-stream EC values in the bark beetle-infested catchments, with particularly elevated EC values during base flow conditions. (Fig. 10) • Associated with the initiation of regeneration in the highly disturbed catchments, EC decreased. • No trend in annual average R and RC in any of the considered catchments.	• Increased EC is caused by the cumulative loading of soil water and groundwater that discharge excess amounts of substances such as nitrogen and carbon, which are released via the decomposition of the needles, branches, and trunks of dead trees, into streams. • Decreased EC is likely caused by vegetative uptake of the excess nitrogen. • The expected runoff increase related to transpiration loss and interception reduction (due to tree mortality) was small or masked by other factors.
Seasonal	• Consistently yielded similar increasing EC trends during all four seasons, in particular the trend is clear in the least disturbed catchment and in the newly disturbed catchment.	
Daily	• Daily EC variability was larger in the least disturbed catchment and in the newly disturbed catchment than two highly disturbed catchments, which was related to elevated instream EC under base flow conditions.	• The mobilization and downward percolation of nutrients and carbon from litter and decomposing needles may be considerable after infestation-induced tree mortality even during moderate rain and infiltration events. • The lack of nutrient uptake by trees could further enhance the cumulative loading of groundwater that discharges into the streams. When the system is flooded under event conditions, substance-enriched soil water and groundwater may be mixed with and diluted by low-salinity event water in a similar manner.
Event	• The positive EC-Q relationships and counter clockwise hysteresis loops were observed in the least disturbed catchment and during the early period of the newly disturbed catchment. • In the highly disturbed catchment, the decreasing EC in response to increasing Q at the beginning of the events as well as the net decrease in in-stream EC during the course of the events	• Healthy forest system required event flows to mobilize substances in the soil and groundwater systems, and a large fractions of total annual in-stream substance loads are released during limited peak flow periods. • When the system is flooded under event conditions, substance-enriched soil water and groundwater may be mixed with and diluted by low-salinity event water, leading to a negative EC-Q relationship.

We placed our study in **Paper III** focusing on understanding the impact of the bark beetle infestation induced land cover change in small catchments within the upper Vydra basin. Four catchments featuring different stages of forest disturbance representing least disturbed catchment, newly disturbed catchment, and two highly disturbed catchments depending on its extent and initial year of the infestation. Our findings (Table 3) were based on statistical analysis using 10min high-frequency 7-year long-term data, and implications of our finding (Table 3) based on theories in **Chapter 3.1, Chapter 3.2, and Chapter 3.3**. We showed the results by different timescales, and we also found that those changes are inter-related. For instance, the infestation-induced changes in event-scale dynamics may be largely responsible for the observed shifts in annual average conditions. A comparison of the EC response patterns of catchments with newly disturbed and those in regions severely infested prior to the monitoring period together proved that hydrogeochemical conditions in the disturbed catchments have relatively long-lasting effects. As the climate-driven bark beetle outbreaks will likely spread in the mid-latitudes, our study provided a better understanding of the mechanisms behind the hydrogeochemical changes in catchments following insect infestation.

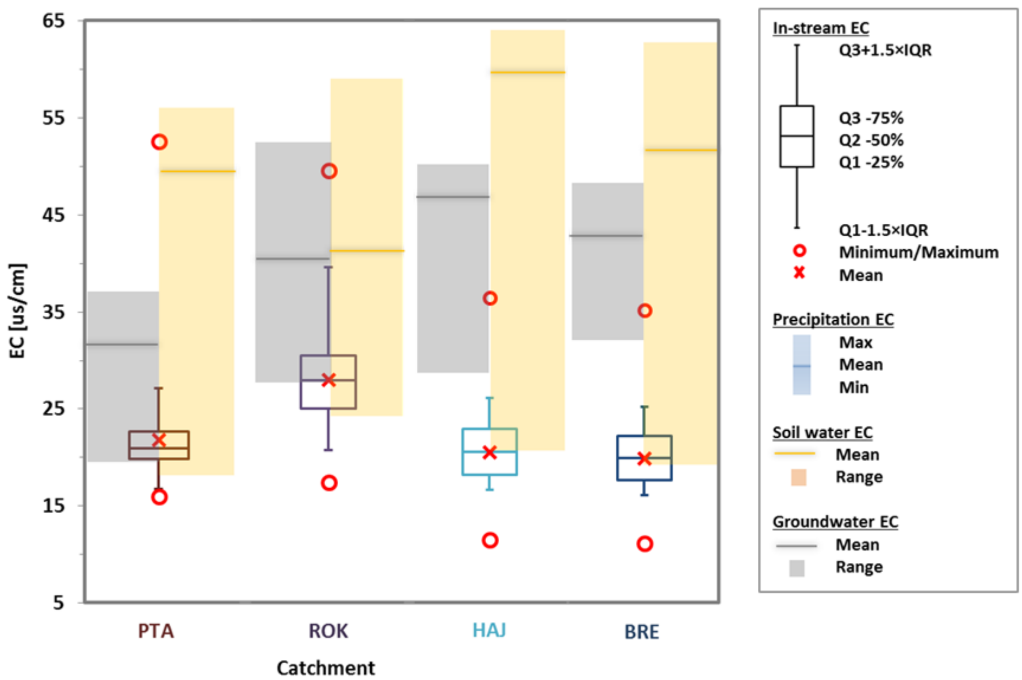

Figure 9. *The EC characteristics in streams, soil, and ground water, and precipitation.*

When implying tracer in the catchment study, we bear in mind that the difference of velocity and celerity for expressing the speed of tracer/mass flow and flood wave was important. Hereafter, we clearly showed a theoretical study in **Paper IV** which provided all useful constitutive relationships under the unit hydraulic gradient condition formulated by the two often-used models - Brooks-Corey model and the modified Mualem -van Genuchten model in Table 4. We highlighted the importance of understanding the tracer transport, which helped us to understand the implications in any tracer-based study, e.g., like study similar as **Paper III**. However, the proposed celerity function is still at the theory stage based on a pore bundle model, which will need more experiments to testify the feasibility to use in the hillslope scale and catchment scales. This theoretical analysis only offered a breakthrough perspective when we using any type of tracer in the water system, to distinguish the flood wave away from the tracer transport.

***Table 4** Constitutive relationships under the unit hydraulic gradient condition formulated by the Brooks-Corey model and the modified Mualem -van Genuchten model*

Property	Definition	Brooks-Corey	Modified Mualem-van Genuchten
Water retention	$\Theta = f(h)$	$\Theta = \begin{cases} \lvert\alpha_{\mathrm{BC}}h\rvert^{-n_{\mathrm{BC}}} , & \alpha_{\mathrm{BC}}h < -1 \\ 1 , & \alpha_{\mathrm{BC}}h > -1 \end{cases}$	$\varepsilon\Theta = \begin{cases} \left[1+\lvert\alpha_{\mathrm{VG}}h\rvert^{n_{\mathrm{VG}}}\right]^{-m_{\mathrm{VG}}} , & h < h_s \\ 1 , & h \geq h_s \end{cases}$
Specific discharge	$q = K$	$K_s\Theta^{\frac{2}{n_{\mathrm{BC}}}+3}$	$K_s\Theta^{l_{\mathrm{VG}}}\left[\dfrac{1-\left(1-(\varepsilon\Theta)^{1/m_{\mathrm{VG}}}\right)^{m_{\mathrm{VG}}}}{1-(1-\varepsilon^{1/m_{\mathrm{VG}}})^{m_{\mathrm{VG}}}}\right]^2$
Average pore velocity	$\bar{v} = \dfrac{q}{\theta-\theta_r}$	$\dfrac{K_s}{\theta_s-\theta_r}\Theta^{\frac{2}{n_{\mathrm{BC}}}+2}$	$\dfrac{K_s}{\theta_s-\theta_r}\Theta^{l_{\mathrm{VG}}-1}\left[\dfrac{1-\left(1-(\varepsilon\Theta)^{1/m_{\mathrm{VG}}}\right)^{m_{\mathrm{VG}}}}{1-\left(1-\varepsilon^{1/m_{\mathrm{VG}}}\right)^{m_{\mathrm{VG}}}}\right]^2$
Celerity	$c = v = \dfrac{dK}{d\theta}$	$\dfrac{a_K K_s}{\theta_s-\theta_r}\Theta^{\frac{2}{n_{\mathrm{BC}}}+2}$	$\dfrac{a_K K_s}{\theta_s-\theta_r}\Theta^{l_{\mathrm{VG}}-1}\left[\dfrac{1-\left(1-(\varepsilon\Theta)^{1/m_{\mathrm{VG}}}\right)^{m_{\mathrm{VG}}}}{1-\left(1-\varepsilon^{1/m_{\mathrm{VG}}}\right)^{m_{\mathrm{VG}}}}\right]^2$
Kinematic ratio	$\alpha_K = c/\bar{v}$	$\dfrac{2}{n_{\mathrm{BC}}}+3$	$l_{\mathrm{VG}} + \dfrac{2\left[1-(\varepsilon\Theta)^{1/m_{\mathrm{VG}}}\right]^{m_{\mathrm{VG}}-1}(\varepsilon\Theta)^{1/m_{\mathrm{VG}}}}{1-\left[1-(\varepsilon\Theta)^{1/m_{\mathrm{VG}}}\right]^{m_{\mathrm{VG}}}}$

Notation of Table: *α (L^{-1}) n (-) and m (-) are the fitting parameters for the Brooks-Corey model (detonated with subscription of "BC") and Mualem-van Genuchten model (detonated with subscription of "VG"); Θ is effective saturation (-) that is defined as: $\Theta = (\theta-\theta_r)/(\theta_s-\theta_r)$; ε is the correction factor to modify the van-Genuchten model $\varepsilon = (\theta_s-\theta_r)/(\theta_m-\theta_r)$, with $\theta_m = \theta_r + (\theta_s-\theta_r)\left[1+\lvert\alpha_{\mathrm{VG}}h_s\rvert^{n_{\mathrm{VG}}}\right]^{m_{\mathrm{VG}}}$, h_s is the minimum capillary height, which becomes zero when $\theta_m = \theta_s$, l_{VG} is pore connectivity parameter, and is usually assumed to be 0.5.*

6.3 Evaporation processes

Estimating evaporation in forest area, the commonly used Penman-Monteith equation coupled with Richards' equation underestimated the total evaporation rate, while a model integrating a non-isothermal multi-phase flow model with a two-layer energy model largely in **Paper V** improved the model accuracy. Our proposed SVAT model was further testified its performance in cropland in **Paper VI** with varying LAI, which helped to examine the model accuracy throughout the entire vegetation period from non-vegetated to LAI=3.2. **Paper VI** proved the importance of considering advective vapour transport in simulating soil moisture content and temperature at the soil surface, which further can affect the simulated evaporation fluxes. An extended study test was conducted for one experimental plot (K2 in

Fig.5 ab) in the upper Vydra basin.

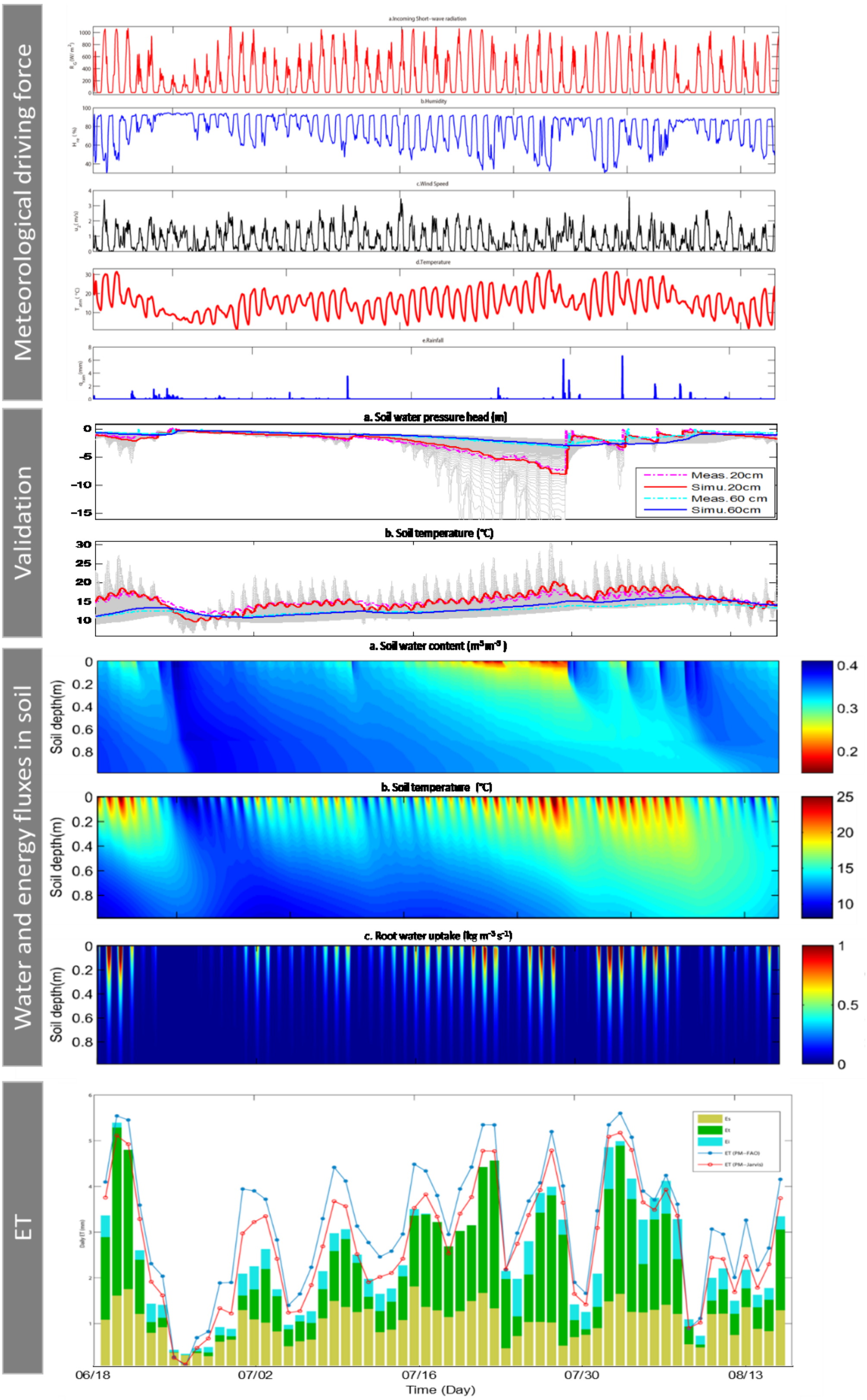

Figure 10. *Simulations of a 2-month vegetation period in the year of 2013 by using our proposed SVAT model.*

The forcing climate data given in Fig. 10a were used in the proposed model for partitioning the evaporating rate. The well-fittings of the soil temperature, and pore water pressure head suggested that the soil physics behaviour was well described by the proposed model. Fig. 10 showed the ability of the model, it can model different components of ET rate, enabling understand the evaporation process in more detail. In particular, such a model would be useful for projecting the future change in such an area with forest disturbance. The functionality of the vegetation under the dry or water deficit condition alters the ET rate, which would be neglected from the simple model. From another perspective, the capacity of vegetation transpiration is lower when there is less water in the soil, consequently, when the temperature increases as projected by climate change models, the total ET amount from the vegetation should decrease. Such an effect will not be considered in any of the simple model for calculating ET.

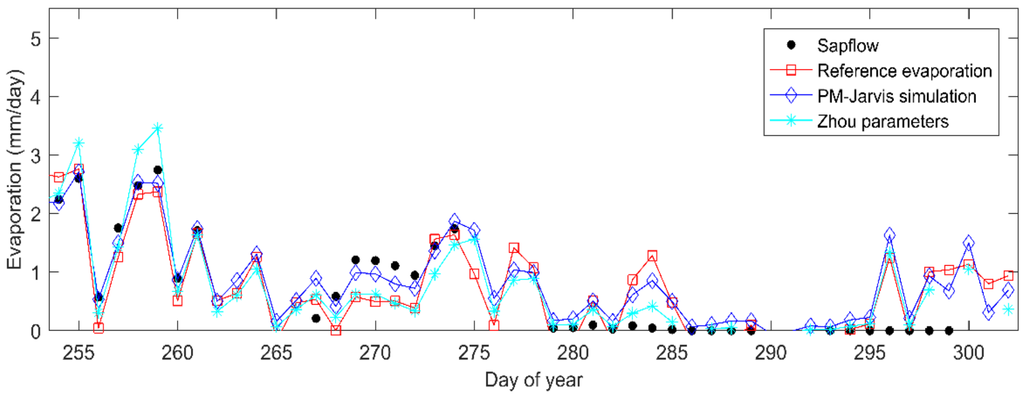

Figure 11. *Stand transpiration measured with sap flow sensors (black dots), evaporation estimated from FAO Penman–Monteith model (i.e. reference evaporation; red square with line), evaporation estimated by PM-JS with calibrated parameters (blue diamond with line), and with Zhou et al. (2006)'s parameters (diamond with line) over DOY 253-DOY 302.*

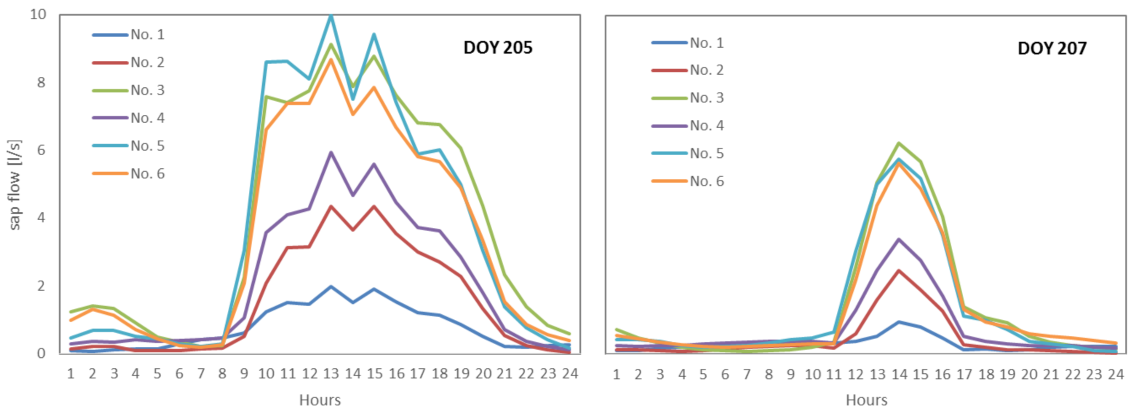

Figure 12. *The diurnal pattern of the measured sap flow in 6 trees (the sizes of the six trees in corresponding numbers are given in Fig. 5c.) at two selected days – DOY 205 and DOY 207.*

During the simulation period, the soil moisture dynamic controls the resistance coefficient of soil surface and foliage stomata resistance (i.e, canopy conductance), and furthermore the energy fluxes of latent heat components. Therefore, we conducted sap flow measurements to understand local transpiration process, and **Paper VII** used sap flow to reversely calculate the canopy conductance and examining the goodness of such a method. We can effectively use calculated conductance to either calculate the evaporation (Fig. 11), and the results show large consistency with the measurements. Such an approach offers a new way to estimate the ET in the area with less monitoring.

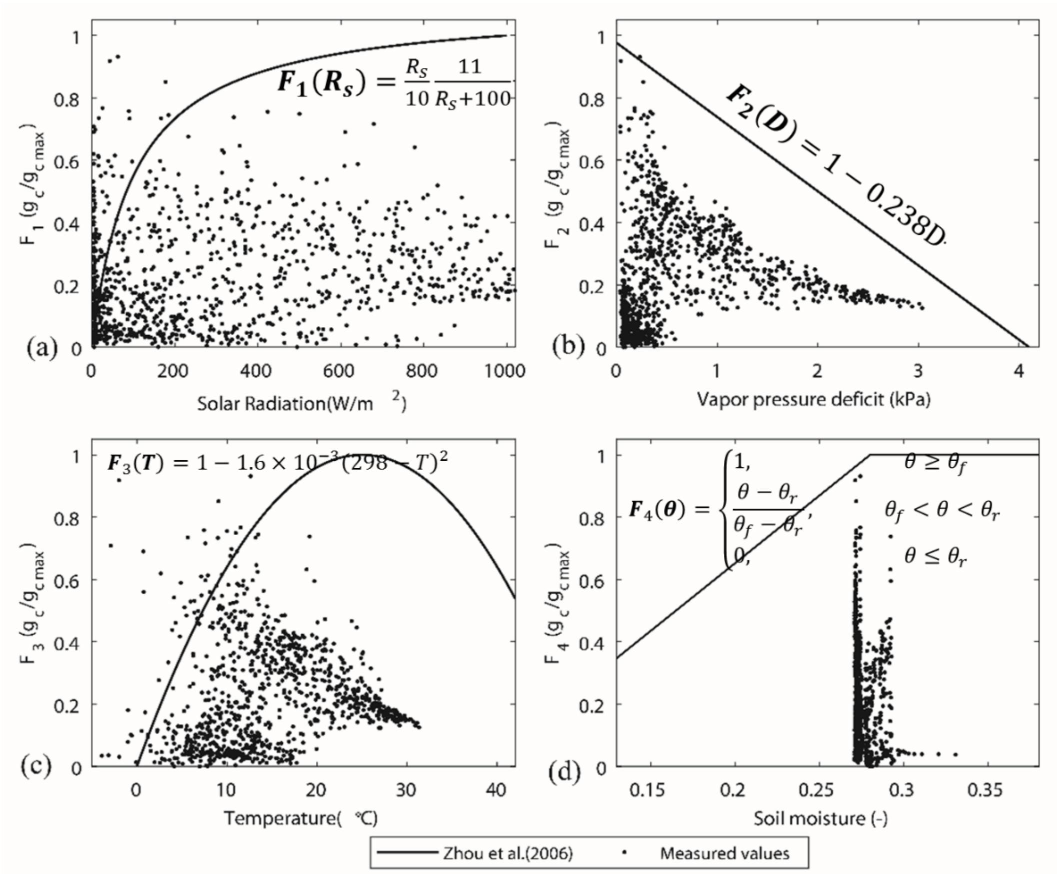

Figure 13. *Response of stress functions in canopy conductance to (**a**) net radiation (Rs), (**b**) vapor pressure deficit (D), (**c**) temperature (T), and (**d**) soil moisture (θ). The line for each sub-figure was using the parameter given by Zhou et al. (2006) and the equation is given on each sub-figure.*

Paper VII also obtained knowledge on the diurnal pattern of the six individual trees with different ages, see Fig. 12. With such information we can classify the forest in the catchment, and calculated the ET in more accurate way. We can observe that there was a drop in transpiration at midday in DOY 205 when it was a sunny day. It can be explained by a limitation of photosynthesis due to the stomatal closure to prevent the water loss from intensive solar radiation and high temperatures. On the contrary, DOY 207 did not show such phenomenon, because the temperature and radiation were not higher than DOY 205. In general, we found that the tree age led to the difference in absolute value of transpiration but the diurnal pattern of this tree species responding to certain climatic conditions are identical, which were used as an evidence for lumping the data for modelling in **Paper VII**.

We here using our measured sap flow data to study the importance of radiation, temperature, vapour pressure deficit, and soil moisture to the canopy conductance (Fig. 13). The response of stomatal conductance showed no pattern with solar radiation and soil moisture, but it did show a clear correlation with the vapour deficit, in particular when explaining the midday drop. The relation to temperature was rather scattered as the measured period was in the moderate climate. Worth mentioning in **Paper VII**, the parameterization of the Jarvis–Stewart model was used to describe the response of stomatal conductance under the varying environmental conditions of net radiation, vapour pressure deficit, temperature, and soil water content (Fig. 13). One important message we got from this study was that the parametrization of stress functions based on the typical deciduous forest does not perfectly represent the measured stomatal response of newly formed beech stands. This finding implies that different environment (even different season in one same area) and different species could lead to different response function of canopy conductance. Therefore, it is necessary to conduct the sap flow measurements in the changing forest after disturbance as the transpiration process might change significantly. This study can provide valuable data to better understanding the evapotranspiration process in newly formed beech stands after the bark beetle outbreak in Central Europe.

7. CONCLUSIONS

The thesis was focused on understanding the hydrological processes and behaviours, which was based on analysing the historical data, developing proper models, and conducting an in-site experiment. Two key study areas were located in two basins of diverting environment in Central Asia and Central Europe, where have different environmental problems but all sharing one common driving factor - climate change. Under the changing climate over nearly half-century, two different environment offered deep insights on how the earth was altered on the hydrological system.

- In the upper Vydra basin (mid-mountain in Central Europe) experiencing forest disturbance and climate change, statistically found even the annual water balance over had no apparent change, regional runoff regime at smaller temporal scale was altered.
- Warmer climate and bark beetle-induced tree mortality in the upper Vydra basin affected **seasonal runoff** (shifted from summers to springs), **occurrence of peak flow events** (doubled since the 1980s with a seasonal shift from late spring towards the early spring), and **occurrence of low flow events** (dropped two-thirds with a seasonal shift from autumn to mid-winter).
- In the Aral Sea Drainage Basin (a semi-arid region in Central Asia, covering 1.3% of the earth's land surface) experiencing intensive agriculture and warmer climate, the **decrease in annual runoff** of the principal river Amu Darya and **an increase of internal recirculation ratio** were found in historical data.
- Climate-driven projections for the ASDB found most likely river flow will **continuously decrease** at the basin outlet, which will **increase internal nutrient recirculation ratios, average transport distances, and attenuation**.

This thesis started from an understanding of the changes in hydrological patterns narrowing down to investigate the specific hydrological processes at smaller spatial and temporal scales, covering studies on the geochemical transformation, tracer transport, and evapotranspiration process. Knowledge and lessons we learnt from theoretical analysis, modelling, and in-site experiment were summarized below.

- Geochemistry at the catchment scale changed over studied 7 years at multi-timescale after bark beetle infestation, and the changes in the disturbed catchments were **rapid after extensive infestation and last long over decades**.
- Along with tree mortality, **increased annual mean in-stream electrical conductivity (EC)** is likely caused by the cumulative loading of soil water and groundwater with substances of nitrogen and carbon released by dead trees. The observed **EC decreases** associated with the initiation of regeneration in the affected catchments was likely caused by vegetative uptake of the excess nitrogen.
- After infestation the **EC-discharge hysteresis loops at the event-scale shifted from positive to negative** relationships, implying changes in the subsurface chemical composition and in the interactions with runoff.

- The proposed **celerity function** has been theoretically proved the usefulness when assist in studying subsurface flow and tracer transport, in particular **the kinematic ratio** (a ratio between celerity and average velocity) could be used to predict the first arrival time of a tracer.
- A **newly proposed model** coupling an SVAT model with a non-isothermal multi-phase flow model was applied in two different environment (forest and maize), and the performance was better due to more detailed description of energy transfer and the formation of advective soil vapour transport.
- **Reversely-calculated canopy conductance** based on **sap flow measurement** had substantially improved the estimation of transpiration during the vegetative period, which can help to better understand the evapotranspiration process in newly form beech stands after bark beetle outbreaks in central Europe.

8. REFERENCES

Abdul AS, Gillham RW. 1989. Field studies of the effects of the capillary fringe on streamflow generation. J. Hydrol., **112**: 1-18. DOI: http://dx.doi.org/10.1016/0022-1694(89)90177-7.

Adam JC, Hamlet AF, Lettenmaier DP. 2009. Implications of global climate change for snowmelt hydrology in the twenty-first century. Hydrological Processes: An International Journal, **23**: 962-972.

Adams HD, Luce CH, Breshears DD, Allen CD, Weiler M, Hale VC, Smith A, Huxman TE. 2012. Ecohydrological consequences of drought-and infestation-triggered tree die-off: insights and hypotheses. Ecohydrology, **5**: 145-159. DOI: 10.1002/eco.233.

Ahmad Z, Hafeez M, Ahmad I. 2012. Hydrology of mountainous areas in the upper Indus Basin, Northern Pakistan with the perspective of climate change. Environ. Monit. Assess., **184**: 5255-5274. DOI: 10.1007/s10661-011-2337-7.

Allan JD. 2004. Landscapes and riverscapes: the influence of land use on stream ecosystems. Annu. Rev. Ecol. Evol. Syst., **35**: 257-284.

Allen RG, Pereira LS, Raes D, Smith M. 1998. Crop evapotranspiration-Guidelines for computing crop water requirements-FAO Irrigation and drainage paper 56. FAO, Rome, **300**: 6541.

Anderson MG, Burt TP. 1978. The role of topography in controlling throughflow generation. Earth Surf. Process., **3**: 331-344. DOI: 10.1002/esp.3290030402.

Arora VK, Boer GJ. 2001. Effects of simulated climate change on the hydrology of major river basins. Journal of Geophysical Research: Atmospheres, **106**: 3335-3348.

Bachmair S, Weiler M. 2012. Hillslope characteristics as controls of subsurface flow variability. Hydrology and Earth System Sciences Discussions, **9**: 6889-6934.

Barnett TP, Adam JC, Lettenmaier DP. 2005. Potential impacts of a warming climate on water availability in snow-dominated regions. Nature, **438**: 303. DOI: 10.1038/nature04141.

Bearup LA, Maxwell RM, Clow DW, McCray JE. 2014. Hydrological effects of forest transpiration loss in bark beetle-impacted watersheds. Nature Clim. Change, **4**: 481-486. DOI: 10.1038/nclimate2198

http://www.nature.com/nclimate/journal/v4/n6/abs/nclimate2198.html#supplementary-information.

Bearup LA, Mikkelson KM, Wiley JF, Navarre-Sitchler AK, Maxwell RM, Sharp JO, McCray JE. 2014. Metal fate and partitioning in soils under bark beetle-killed trees. Sci. Tot. Environ., **496**: 348-357.

Beniston M. 2003. Climatic change in mountain regions: a review of possible impacts. In: Climate variability and change in high elevation regions: Past, present & future, Springer, pp: 5-31.

Bentz BJ, Régnière J, Fettig CJ, Hansen EM, Hayes JL, Hicke JA, Kelsey RG, Negrón JF, Seybold SJ. 2010. Climate change and bark beetles of the western United States and Canada: direct and indirect effects. BioScience, **60**: 602-613. DOI: http://dx.doi.org/10.1525/bio.2010.60.8.6.

Berg EE, Henry JD, Fastie CL, De Volder AD, Matsuoka SM. 2006. Spruce beetle outbreaks on the Kenai Peninsula, Alaska, and Kluane National Park and Reserve, Yukon Territory: relationship to summer temperatures and regional differences in disturbance regimes. Forest Ecology and Management, **227**: 219-232. DOI: doi:10.1016/j.foreco.2006.02.038.

Beudert B, Klöcking B, Marcq B, Niederberger J, Puhlmann H, Schwarze R, Wilpert K-Hv. 2007. Forest hydrology-results of research in Germany and Russia. In: Part I Results of research in Germany, Puhlmann H, Schwarze R (eds.) ihp.hwrp Germany, pp: 131.

Beven K. 1981. Kinematic subsurface stormflow. Water Resources Research, **17**: 1419-1424. DOI: http://dx.doi.org/10.1029/WR017i005p01419.

Beven K. 1989. Changing ideas in hydrology — The case of physically-based models. Journal of Hydrology, **105**: 157-172. DOI: http://dx.doi.org/10.1016/0022-1694(89)90101-7.

Beven K, Germann P. 1982. Macropores and water flow in soils. Water Resour. Res., **18**: 1311-1325.

Beven K, Germann P. 2013. Macropores and water flow in soils revisited. Water Resources Research, **49**: 3071-3092. DOI: http://dx.doi.org/10.1002/wrcr.20156.

Beven K, Kirkby M. 1979. A physically based, variable contributing area model of basin hydrology/Un modèle à base physique de zone d'appel variable de l'hydrologie du bassin versant. Hydrol. Sci. J., **24**: 43-69.

Beven KJ. 2010. Preferential flows and travel time distributions: defining adequate hypothesis tests for hydrological process models. Hydrol. Processes, **24**: 1537-1547.

Birsan M-V, Molnar P, Burlando P, Pfaundler M. 2005. Streamflow trends in Switzerland. J. Hydrol., **314**: 312-329. DOI: http://dx.doi.org/10.1016/j.jhydrol.2005.06.008.

Bishop K, Seibert J, Köhler S, Laudon H. 2004. Resolving the Double Paradox of rapidly mobilized old water with highly variable responses in runoff chemistry. Hydrol. Processes, **18**: 185-189. DOI: 10.1002/hyp.5209.

Blume T, Zehe E, Bronstert A. 2007. Rainfall—runoff response, event-based runoff coefficients and hydrograph separation. Hydrol. Sci. J., **52**: 843-862.

Blyth E, Harding RJ. 2011. Methods to separate observed global evapotranspiration into the interception, transpiration and soil surface evaporation components. Hydrological Processes, **25**: 4063-4068. DOI: 10.1002/hyp.8409.

Bonell M. 1998. SELECTED CHALLENGES IN RUNOFF GENERATION RESEARCH IN FORESTS FROM THE HILLSLOPE TO HEADWATER DRAINAGE BASIN SCALE1. JAWRA Journal of the American Water Resources Association, **34**: 765-785. DOI: 10.1111/j.1752-1688.1998.tb01514.x.

Bonell M, Gilmour DA. 1978. The development of overland flow in a tropical rainforest catchment. J. Hydrol., **39**: 365-382. DOI: http://dx.doi.org/10.1016/0022-1694(78)90012-4.

Bosch JM, Hewlett JD. 1982. A review of catchment experiments to determine the effect of vegetation changes on water yield and evapotranspiration. J. Hydrol., **55**: 3-23. DOI: http://dx.doi.org/10.1016/0022-1694(82)90117-2.

Botter G, Bertuzzo E, Rinaldo A. 2010. Transport in the hydrologic response: Travel time distributions, soil moisture dynamics, and the old water paradox. Water Resour. Res., **46**: W03514. DOI: 10.1029/2009WR008371.

Botter G, Peratoner F, Putti M, Zuliani A, Zonta R, Rinaldo A, Marani M. 2008. Observation and modeling of catchment-scale solute transport in the hydrologic response: A tracer study. Water Resour. Res., **44**: W05409. DOI: 10.1029/2007WR006611.

Bronstert A, Niehoff D, Burger G. 2002. Effects of climate and land-use change on storm runoff generation: present knowledge and modelling capabilities. Hydrol. Processes, **16**: 509-529. DOI: Doi 10.1002/Hyp.326.

Browder JO. 2002. The urban-rural interface: Urbanization and tropical forest cover change. Urban Ecosyst., **6**: 21-41.

Brusseau M, Rao P. 1990. Modeling solute transport in structured soils: A review. Geoderma, **46**: 169-192.

Bullock A, Acreman M. 1999. The role of wetlands in the hydrological cycle. Hydrol. Earth Syst. Sci., **7**: 358-389.

Burns DA, McDonnell JJ, Hooper RP, Peters NE, Freer JE, Kendall C, Beven K. 2001. Quantifying contributions to storm runoff through end-member mixing analysis and hydrologic measurements at the Panola Mountain Research Watershed (Georgia, USA). Hydrol. Processes, **15**: 1903-1924. DOI: 10.1002/hyp.246.

Buttle J. 1994. Isotope hydrograph separations and rapid delivery of pre-event water from drainage basins. Prog. Phys. Geog., **18**: 16-41.

Buttle JM, Metcalfe RA. 2000. Boreal forest disturbance and streamflow response, northeastern Ontario. Canadian Journal of Fisheries and Aquatic Sciences, **57**: 5-18. DOI: 10.1139/cjfas-57-S2-5.

Cainelli O, Bellin A, Putti M. 2012. On the accuracy of classic numerical schemes for modeling flow in saturated heterogeneous formations. Advances in Water Resources, **47**: 43-55. DOI: http://dx.doi.org/10.1016/j.advwatres.2012.06.016.

Carlson TN, Arthur ST. 2000. The impact of land use—land cover changes due to urbanization on surface microclimate and hydrology: a satellite perspective. Global Planet. Change, **25**: 49-65.

Christensen JH, Carter TR, Rummukainen M, Amanatidis G. 2007. Evaluating the performance and utility of regional climate models: the PRUDENCE project. Clim. Change, **81**: 1-6.

Clow DW, Rhoades C, Briggs J, Caldwell M, Lewis Jr WM. 2011. Responses of soil and water chemistry to mountain pine beetle induced tree mortality in Grand County, Colorado, USA. Appl. Geochem., **26**: S174-S178.

D'Odorico P, Fagherazzi S, Rigon R. 2005. Potential for landsliding: Dependence on hyetograph characteristics. Journal of Geophysical Research: Earth Surface, **110**: F01007. DOI: 10.1029/2004JF000127.

Dale VH, Joyce LA, McNulty S, Neilson RP, Ayres MP, Flannigan MD, Hanson PJ, Irland LC, Lugo AE, Peterson CJ. 2001. Climate change and forest disturbances: climate change can affect forests by altering the frequency, intensity, duration, and timing of fire, drought, introduced species, insect and pathogen outbreaks, hurricanes, windstorms, ice storms, or landslides. AIBS Bulletin, **51**: 723-734.

Dam JC. 1999. Impacts of Climate Change and Variability on Hydrological Regimes. Cambridge Univeristy Press.

Dunne T. 1978. Field studies of hillslope flow processes. . In: In Hillslope Hydrology, MJ. K (ed.) Wiley, pp: 227-293.

Durner W, Flühler H. 1996. Multi-domain model for pore-size dependent transport of solutes in soils. Geoderma, **70**: 281-297.

Eckhardt K, Ulbrich U. 2003. Potential impacts of climate change on groundwater recharge and streamflow in a central European low mountain range. J. Hydrol., **284**: 244-252. DOI: https://doi.org/10.1016/j.jhydrol.2003.08.005.

Edburg SL, Hicke JA, Brooks PD, Pendall EG, Ewers BE, Norton U, Gochis D, Gutmann ED, Meddens AJ. 2012. Cascading impacts of bark beetle-caused tree mortality on coupled biogeophysical and biogeochemical processes. Frontiers in Ecology and the Environment, **10**: 416-424.

Eltahir EAB. 1998. A soil moisture-rainfall feedback mechanism. 1. Theory and observations. Water Resour. Res., **34**: 765-776.

Eltahir EAB. 1998. A Soil Moisture–Rainfall Feedback Mechanism: 1. Theory and observations. Water Resources Research, **34**: 765-776. DOI: 10.1029/97WR03499.

Entekhabi D, Rodriguez-Iturbe I, Castelli F. 1996. Mutual interaction of soil moisture state and atmospheric processes. Journal of Hydrology, **184**: 3-17. DOI: http://dx.doi.org/10.1016/0022-1694(95)02965-6.

Ewers B, Gower S, Bond-Lamberty B, Wang C. 2005. Effects of stand age and tree species on canopy transpiration and average stomatal conductance of boreal forests. Plant, Cell & Environment, **28**: 660-678.

Feddema JJ, Oleson KW, Bonan GB, Mearns LO, Buja LE, Meehl GA, Washington WM. 2005. The importance of land-cover change in simulating future climates. Science, **310**: 1674-1678.

Feng Y, Yoshinaga I, Shiratani E, Hitomi T, Hasebe H. 2004. Characteristics and behavior of nutrients in a paddy field area equipped with a recycling irrigation system. Agricultural water management, **68**: 47-60.

Flühler H, Durner W, Flury M. 1996. Lateral solute mixing processes—A key for understanding field-scale transport of water and solutes. Geoderma, **70**: 165-183.

Foley JA, DeFries R, Asner GP, Barford C, Bonan G, Carpenter SR, Chapin FS, Coe MT, Daily GC, Gibbs HK. 2005. Global consequences of land use. Science, **309**: 570-574.

Ford CR, Vose JM. 2007. Tsuga canadensis (L.) Carr. mortality will impact hydrologic processes in southern Appalachian forest ecosystems. Ecological Applications, **17**: 1156-1167.

Freer J, J. MJ, J. BK, E. PN, A. BD, P. HR, B. A, C. K. 2002. The role of bedrock topography on subsurface storm flow. Water Resources Research, **38**: 5-1-5-16. DOI: doi:10.1029/2001WR000872.

Freer J, McDonnell JJ, Beven KJ, Peters NE, Burns DA, Hooper RP, Aulenbach B, Kendall C. 2002. The role of bedrock topography on subsurface storm flow. Water Resources Research, **38**: 1269. DOI: 10.1029/2001WR000872.

Freeze RA. 1972. Role of subsurface flow in generating surface runoff: 1. Base flow contributions to channel flow. Water Resour. Res., **8**: 609-623. DOI: 10.1029/WR008i003p00609.

Gannon JP, Bailey SW, McGuire KJ. 2014. Organizing groundwater regimes and response thresholds by soils: A framework for understanding runoff generation in a headwater catchment. Water Resour. Res., **50**: 8403-8419. DOI: 10.1002/2014WR015498.

Geris J, Tetzlaff D, McDonnell J, Soulsby C. 2014. The relative role of soil type and tree cover on water storage and transmission in northern headwater catchments. Hydrol. Processes: n/a-n/a. DOI: 10.1002/hyp.10289.

Gordon LJ, Peterson GD, Bennett EM. 2008. Agricultural modifications of hydrological flows create ecological surprises. Trends in Ecology & Evolution, **23**: 211-219.

Gran M, Carrera J, Olivella S, Saaltink MW. 2011. Modeling evaporation processes in a saline soil from saturation to oven dry conditions. Hydrol. Earth Syst. Sci., **15**: 2077-2089. DOI: 10.5194/hess-15-2077-2011.

Granier A, Biron P, Lemoine D. 2000. Water balance, transpiration and canopy conductance in two beech stands. Agricultural and forest meteorology, **100**: 291-308.

Grau HR, Gasparri NI, Aide TM. 2005. Agriculture expansion and deforestation in seasonally dry forests of north-west Argentina. Environ. Conserv., **32**: 140-148.

Gundersen P, Schmidt IK, Raulund-Rasmussen K. 2006. Leaching of nitrate from temperate forests effects of air pollution and forest management. Environmental reviews, **14**: 1-57.

H.Gleick P. 1989. Climate change, hydrology, and water resources. Rev. Geophys., **27**: 329-344. DOI: doi:10.1029/RG027i003p00329.

Haidary A, Amiri BJ, Adamowski J, Fohrer N, Nakane K. 2013. Assessing the Impacts of Four Land Use Types on the Water Quality of Wetlands in Japan. Water Resour. Manage., **27**: 2217-2229. DOI: 10.1007/s11269-013-0284-5.

Hais M, Jonášová M, Langhammer J, Kučera T. 2009. Comparison of two types of forest disturbance using multitemporal Landsat TM/ETM+ imagery and field vegetation data. Remote Sens. Environ., **113**: 835-845. DOI: http://dx.doi.org/10.1016/j.rse.2008.12.012.

Hangen E, Lindenlaub M, Leibundgut C, von Wilpert K. 2001. Investigating mechanisms of stormflow generation by natural tracers and hydrometric data: a small catchment study in the Black Forest, Germany. Hydrol. Processes, **15**: 183-199. DOI: 10.1002/hyp.142.

Hauer FR, Lorang MS. 2004. River regulation, decline of ecological resources, and potential for restoration in a semi-arid lands river in the western USA. Aquat. Sci., **66**: 388-401.

Hewlett JD, Hibbert AR. 1967. Factors affecting the response of small watersheds to precipitation in humid areas. Forest hydrology: 275-290.

Hill J, Hamer K, Lace L, Banham W. 1995. Effects of selective logging on tropical forest butterflies on Buru, Indonesia. Journal of Applied Ecology: 754-760.

Hitomi T, Yoshinaga I, Feng Y, Shiratani E. 2006. Nitrogen removal function of recycling irrigation system. Water Sci. Technol., **53**: 101-109.

Hornbeck JW, Pierce RS, Federer CA. 1970. Streamflow Changes after Forest Clearing in New England. Water Resour. Res., **6**: 1124-1132. DOI: 10.1029/WR006i004p01124.

Horton RE. 1933. The role of infiltration in the hydrologic cycle. Transactions, American Geophysical Union, **14**: 446-460.

Houghton R. 1999. The annual net flux of carbon to the atmosphere from changes in land use 1850–1990. Tellus B, **51**: 298-313.

Hrachowitz M, Savenije H, Bogaard T, Tetzlaff D, Soulsby C. 2013. What can flux tracking teach us about water age distribution patterns and their temporal dynamics. Hydrol. Earth Syst. Sci, **17**: 533-564.

Huber C, Baumgarten M, Göttlein A, Rotter V. 2004. Nitrogen turnover and nitrate leaching after bark beetle attack in mountainous spruce stands of the Bavarian Forest National Park. Water, Air and Soil Pollution: Focus, **4**: 391-414.

Ilhardt BL, Verry ES, Palik BJ. 2000. Defining riparian areas. FORESTRY AND THE RIPARIAN ZONE: 7.

IPCC. 2007. Climate Change 2007: The Physical Science Basis. In: Contribution of Working Group I to the Fourth Assessment Report of the Intergovernmental Panel on Climate Change, 2007, Solomon S, Qin D, Manning M, Chen Z, Marquis M, Averyt KB, Tignor M, Miller HL (eds.) Cambridge University Press,, pp: 996.

IPCC. 2013. Climate Change 2013: The Physical Science Basis. In: Contribution of Working Group I to the Fifth Assessment Report of the Intergovernmental Panel on Climate Change, Stocker TF, D. Qin, G.-K. Plattner, M. Tignor, S.K. Allen, J. Boschung, A. Nauels, Y. Xia, V. Bex and P.M. Midgley (ed.), pp: 1535.

Jarsjö J, Asokan S, Prieto C, Bring A, Destouni G. 2011. Hydrological responses to climate change conditioned by historic alterations of land-use and water-use. Hydrology & Earth System Sciences Discussions, **8**.

Jarsjö J, Asokan SM, Prieto C, Bring A, Destouni G. 2012. Hydrological responses to climate change conditioned by historic alterations of land-use and water-use. Hydrol. Earth Syst. Sci., **16**: 1335-1347.

Jarsjö J, Asokan, S. M., Prieto, C., Bring, A., and Destouni, G. 2012. Hydrological responses to climate change conditioned by historic alterations of land-use and water-use. Hydrol. Earth Syst. Sci., **16**: 1335-1347. DOI: https://doi.org/10.5194/hess-16-1335-2012.

Jarsjö J, Törnqvist R, Su Y. 2017. Climate-driven change of nitrogen retention–attenuation near irrigated fields: multi-model projections for Central Asia. Environ Earth Sci, **76**: 117.

Jørgensen SE. 2016. Ecohydrology as an important concept and tool in environmental management. Ecohydrology & Hydrobiology, **16**: 4-6. DOI: https://doi.org/10.1016/j.ecohyd.2015.04.005.

Kaimowitz D. 1996. Livestock and deforestation in Central America in the 1980s and 1990s: a policy perspective. Cifor.

Kalnay E, Cai M. 2003. Impact of urbanization and land-use change on climate. Nature, **423**: 528.

Kampf SK, Burges SJ. 2007. A framework for classifying and comparing distributed hillslope and catchment hydrologic models. Water Resources Research, **43**: W05423. DOI: 10.1029/2006WR005370.

Kaňa J, Tahovská K, Kopáček J. 2013. Response of soil chemistry to forest dieback after bark beetle infestation. Biogeochemistry, **113**: 369-383.

Kendall KA, Shanley J, McDonnell JJ. 1999. A hydrometric and geochemical approach to test the transmissivity feedback hypothesis during snowmelt. Journal of Hydrology, **219**: 188-205.

Khaledian Y, Kiani F, Sohaila E. 2012. The effect of land use change on soil and water quality in northern Iran. Journal of Mountain Science, **9**: 798-816. DOI: 10.1007/s11629-012-2301-1.

Kliment Z, Matouskova M, Ledvinka O, Kralovec V. 2011. Trend Analysis of Rainfall-Runoff Regimes in Selected Headwater Areas of the Czech Republic. J. Hydrol. Hydromech., **59**: 36-50. DOI: DOI 10.2478/v10098-011-0003-y.

Köhne JM, Köhne S, Šimůnek J. 2009. A review of model applications for structured soils: a) Water flow and tracer transport. J. Contam. Hydrol., **104**: 4-35.

Kotb TH, Watanabe T, Ogino Y, Tanji KK. 2000. Soil salinization in the Nile Delta and related policy issues in Egypt. Agricultural water management, **43**: 239-261.

Kriaučiūnien J, Šarauskien D, Gailiušis B. 2009. Estimation of Uncertainty in Catchment–Scale Modeling of Climate Change Impact (Case of the Merkys River, Lithuania). Environmental Research, Engineering and Management, **1**: 30-39.

Kuang X, Jiao JJ, Li H. 2013. Review on airflow in unsaturated zones induced by natural forcings. Water Resources Research, **49**: 6137-6165. DOI: 10.1002/wrcr.20416.

Kurz WA, Dymond C, Stinson G, Rampley G, Neilson E, Carroll A, Ebata T, Safranyik L. 2008. Mountain pine beetle and forest carbon feedback to climate change. Nature, **452**: 987.

Lambin EF, Geist HJ, Lepers E. 2003. Dynamics of land-use and land-cover change in tropical regions. Annual review of environment and resources, **28**: 205-241.

Langhammer J, Su Y, Bernsteinová J. 2015. Runoff response to climate warming and forest disturbance in a mid-mountain basin. Water, **7**: 3320-3342.

Laudon H, Slaymaker O. 1997. Hydrograph separation using stable isotopes, silica and electrical conductivity: an alpine example. J. Hydrol., **201**: 82-101.

Lawrence DM, Thornton PE, Oleson KW, Bonan GB. 2007. The Partitioning of Evapotranspiration into Transpiration, Soil Evaporation, and Canopy Evaporation in a GCM: Impacts on Land–Atmosphere Interaction. Journal of Hydrometeorology, **8**: 862-880. DOI: 10.1175/JHM596.1.

Liang X, Lettenmaier DP, Wood EF, Burges SJ. 1994. A simple hydrologically based model of land surface water and energy fluxes for general circulation models. Journal of Geophysical Research: Atmospheres (1984–2012), **99**: 14415-14428.

Lin Y-S, Medlyn BE, Duursma RA, Prentice IC, Wang H, Baig S, Eamus D, de Dios VR, Mitchell P, Ellsworth DS. 2015. Optimal stomatal behaviour around the world. Nature Climate Change, **5**: 459-464.

Lioubimtseva E, Henebry G. 2009. Climate and environmental change in arid Central Asia: Impacts, vulnerability, and adaptations.

Lioubimtseva E, Henebry GM. 2009. Climate and environmental change in arid Central Asia: Impacts, vulnerability, and adaptations. J. Arid Environ., **73**: 963-977.

Ma X, Xu J, van Noordwijk M. 2010. Sensitivity of streamflow from a Himalayan catchment to plausible changes in land cover and climate. Hydrol. Processes, **24**: 1379-1390. DOI: 10.1002/hyp.7602.

Manabe S, Stouffer RJ. 1980. Sensitivity of a global climate model to an increase of CO2 concentration in the atmosphere. Journal of Geophysical Research: Oceans, **85**: 5529-5554.

Matthews E. 1983. Global vegetation and land use: New high-resolution data bases for climate studies. J. Clim. Appl. Meteorol., **22**: 474-487.

McDonnell JJ. 2003. Where does water go when it rains? Moving beyond the variable source area concept of rainfall-runoff response. Hydrol. Processes, **17**: 1869-1875.

McDonnell JJ, Beven K. 2014. Debates—The future of hydrological sciences: A (common) path forward? A call to action aimed at understanding velocities, celerities and residence time distributions of the headwater hydrograph. Water Resour. Res.

McDonnell JJ, Beven K. 2014. Debates—The future of hydrological sciences: A (common) path forward? A call to action aimed at understanding velocities, celerities and residence time distributions of the headwater hydrograph. Water Resources Research, **50**: 5342-5350. DOI: 10.1002/2013wr015141.

McGuire K, McDonnell J, Weiler M, Kendall C, McGlynn B, Welker J, Seibert J. 2005. The role of topography on catchment-scale water residence time. Water Resour. Res., **41**.

Micklin P. 2007. The Aral sea disaster. Annu. Rev. Earth Planet. Sci., **35**: 47-72.

Mikkelson KM, Bearup LA, Maxwell RM, Stednick JD, McCray JE, Sharp JO. 2013. Bark beetle infestation impacts on nutrient cycling, water quality and interdependent hydrological effects. Biogeochemistry, **115**: 1-21.

Mikkelson KM, Dickenson ER, Maxwell RM, McCray JE, Sharp JO. 2013. Water-quality impacts from climate-induced forest die-off. Nature Climate Change, **3**: 218.

Milly PC, Dunne KA, Vecchia AV. 2005. Global pattern of trends in streamflow and water availability in a changing climate. Nature, **438**: 347.

Moene AF, van Dam JC. 2014. Transport in the Atmosphere-vegetation-soil Continuum. Cambridge University Press.

Monteith J, Unsworth M. 2013. Principles of Environmental Physics: Plants, Animals, and the Atmosphere. Academic Press.

Moore RD, Richards G, Story A. 2008. Electrical Conductivity as an Indicator of Water Chemistry and Hydrologic Process. Streamline Watershed Management Bulletin, **11**: 25-29.

Muñoz-Villers LE, McDonnell JJ. 2013. Land use change effects on runoff generation in a humid tropical montane cloud forest region. Hydrol. Earth Syst. Sci., **17**: 3543-3560. DOI: 10.5194/hess-17-3543-2013.

Muñoz-Villers LE, McDonnell JJ. 2012. Runoff generation in a steep, tropical montane cloud forest catchment on permeable volcanic substrate. Water Resour. Res., **48**.

Naiman RJ, Décamps H. 1997. The ecology of interfaces: riparian zones. Annual review of Ecology and Systematics: 621-658.

Nakamura R. 1971. Runoff analysis by electrical conductance of water. J. Hydrol., **14**: 197-212.

Nicótina L, Alessi Celegon E, Rinaldo A, Marani M. 2008. On the impact of rainfall patterns on the hydrologic response. Water Resour. Res., **44**: W12401. DOI: 10.1029/2007WR006654.

Nieber JL, Sidle RC. 2010. How do disconnected macropores in sloping soils facilitate preferential flow? Hydrological Processes, **24**: 1582-1594. DOI: http://dx.doi.org/10.1002/hyp.7633.

Nielsen DR, Th. Van Genuchten M, Biggar JW. 1986. Water flow and solute transport processes in the unsaturated zone. Water Resources Research, **22**: 89S-108S. DOI: 10.1029/WR022i09Sp0089S.

Palmer MA, Reidy Liermann CA, Nilsson C, Flörke M, Alcamo J, Lake PS, Bond N. 2008. Climate change and the world's river basins: anticipating management options. Frontiers in Ecology and the Environment, **6**: 81-89.

Park YJ, Sudicky EA, Brookfield AE, Jones JP. 2011. Hydrologic response of catchments to precipitation: Quantification of mechanical carriers and origins of water. Water Resour. Res., **47**: W12515. DOI: 10.1029/2010WR010075.

Pellerin BA, Wollheim WM, Feng X, Vörösmarty CJ. 2008. The application of electrical conductivity as a tracer for hydrograph separation in urban catchments. Hydrol. Processes, **22**: 1810-1818.

Phillips FM. 2010. Hydrology: Soil-water bypass. Nat. Geosci., **3**: 77-78.

Pielke RA. 2005. Land use and climate change. Science, **310**: 1625-1626.

Pinder GF, Jones JF. 1969. Determination of the ground-water component of peak discharge from the chemistry of total runoff. Water Resour. Res., **5**: 438-445. DOI: 10.1029/WR005i002p00438.

Pomeroy J, Fang X, Ellis C. 2012. Sensitivity of snowmelt hydrology in Marmot Creek, Alberta, to forest cover disturbance. Hydrol. Processes, **26**: 1891-1904. DOI: 10.1002/hyp.9248.

Qi J, Kulmatov R. 2008. An overview of environmental issues in Central Asia. In: Environmental Problems of Central Asia and their Economic, Social and Security Impacts, Springer, pp: 3-14.

Rao P, Agaewal S. 1984. Diurnal variation in leaf water potential, stomatal conductance, and irradiance of winter crop under different moisture levels. Biologia plantarum, **26**: 1-4.

Redding T, Winkler R, Teti P, Spittlehouse D, Boon S, Rex J, Dubé S, Moore R, Wei A, Carver M. 2008. Mountain pine beetle and watershed hydrology. In: Mountain pine beetle: From lessons learned to community-based solutions Conference Proceedings, June 10–11, 2008. BC Journal of Ecosystems and Management 9 (3): 33–50. www. forrex. org/publications/jem/ISS49/vol9_no3_MPBconference. pdf (Accessed August 2009).

Reed DE, Ewers BE, Pendall E. 2014. Impact of mountain pine beetle induced mortality on forest carbon and water fluxes. Environmental Research Letters, **9**: 105004.

Rice KC, Hornberger GM. 1998. Comparison of hydrochemical tracers to estimate source contributions to peak flow in a small, forested, headwater catchment. Water Resour. Res., **34**: 1755-1766.

Ridler M-E, Madsen H, Stisen S, Bircher S, Fensholt R. 2014. Assimilation of SMOS-derived soil moisture in a fully integrated hydrological and soil-vegetation-atmosphere transfer model in Western Denmark. Water Resources Research, **50**: 8962-8981. DOI: doi:10.1002/2014WR015392.

Roberts J. 2000. The influence of physical and physiological characteristics of vegetation on their hydrological response. Hydrological Processes, **14**: 2885-2901.

Robinson C, Tockner K, Ward J. 2002. The fauna of dynamic riverine landscapes. Freshwater Biology, **47**: 661-677.

Rodriguez-Iturbe I. 2000. Ecohydrology: A hydrologic perspective of climate-soil-vegetation dynamies. Water Resources Research, **36**: 3-9. DOI: 10.1029/1999WR900210.

Saiko TA, Zonn IS. 2000. Irrigation expansion and dynamics of desertification in the Circum-Aral region of Central Asia. Appl. Geog., **20**: 349-367. DOI: https://doi.org/10.1016/S0143-6228(00)00014-X.

Savenije H. 2010. HESS Opinions" Topography driven conceptual modelling (FLEX-Topo)". Hydrol. Earth Syst. Sci., **14**: 2681-2692.

Savenije HHG. 2004. The importance of interception and why we should delete the term evapotranspiration from our vocabulary. Hydrological Processes, **18**: 1507-1511. DOI: 10.1002/hyp.5563.

Seibert J, Bishop K, Rodhe A, McDonnell JJ. 2003. Groundwater dynamics along a hillslope: A test of the steady state hypothesis. Water Resour. Res., **39**: 1014. DOI: 10.1029/2002WR001404.

Seidl R, SCHELHAAS MJ, Lexer MJ. 2011. Unraveling the drivers of intensifying forest disturbance regimes in Europe. Global Change Biology, **17**: 2842-2852.

Seidl R, Thom D, Kautz M, Martin-Benito D, Peltoniemi M, Vacchiano G, Wild J, Ascoli D, Petr M, Honkaniemi J. 2017. Forest disturbances under climate change. Nature climate change, **7**: 395.

Seneviratne SI, Corti T, Davin EL, Hirschi M, Jaeger EB, Lehner I, Orlowsky B, Teuling AJ. 2010. Investigating soil moisture–climate interactions in a changing climate: A review. Earth-Science Reviews, **99**: 125-161. DOI: http://dx.doi.org/10.1016/j.earscirev.2010.02.004.

Shibuo Y, Jarsjö J, Destouni G. 2007. Hydrological responses to climate change and irrigation in the Aral Sea drainage basin. Geophys. Res. Lett., **34**.

Singh VP. 2002. Is hydrology kinematic? Hydrological Processes, **16**: 667-716. DOI: 10.1002/hyp.306.

Sklash MG, Farvolden RN. 1979. The role of groundwater in storm runoff. Developments in Water Science, **12**: 45-65.

Sklash MG, Stewart MK, Pearce AJ. 1986. Storm Runoff Generation in Humid Headwater Catchments: 2. A Case Study of Hillslope and Low-Order Stream Response. Water Resour. Res., **22**: 1273-1282. DOI: 10.1029/WR022i008p01273.

Sorg A, Bolch T, Stoffel M, Solomina O, Beniston M. 2012. Climate change impacts on glaciers and runoff in Tien Shan (Central Asia). Nature Climate Change, **2**: 725. DOI: 10.1038/nclimate1592

https://www.nature.com/articles/nclimate1592#supplementary-information.

Stow DA, Hope A, McGuire D, Verbyla D, Gamon J, Huemmrich F, Houston S, Racine C, Sturm M, Tape K. 2004. Remote sensing of vegetation and land-cover change in Arctic Tundra Ecosystems. Remote Sens. Environ., **89**: 281-308.

Su Y, Langhammer J. 2014. FEASIBILITY OF USING A SALT TRACER DILUTION METHOD TO ESTIMATE STREAM FLOW IN SMALL MOUNTAINOUS CATCHMENTS IN THE SUMAVA MOUNTAINS. In: CER Comparative European Research 2014 Michael McGreevy RR (ed.) Sciemcee Publishing, pp: 106-109.

Su Y, Langhammer J, Jarsjö J. 2017. Geochemical responses of forested catchments to bark beetle infestation: Evidence from high frequency in-stream electrical conductivity monitoring. J. Hydrol., **550**: 635-649.

Su Y, Shao W, Vlček L, Langhammer J. 2019. Ecohydrological Behaviour of Mountain Beech Forest: Quantification of Stomatal Conductance Using Sap Flow Measurements. Geosciences, **9**: 243.

Takeda I, Fukushima A, Tanaka R. 1997. Non-point pollutant reduction in a paddy-field watershed using a circular irrigation system. Water Res., **31**: 2685-2692.

Tetzlaff D, Birkel C, Dick J, Geris J, Soulsby C. 2014. Storage dynamics in hydropedological units control hillslope connectivity, runoff generation, and the evolution of catchment transit time distributions. Water Resour. Res., **50**: 969-985. DOI: 10.1002/2013WR014147.

Tilman D. 1999. Global environmental impacts of agricultural expansion: the need for sustainable and efficient practices. Proceedings of the National Academy of Sciences, **96**: 5995-6000.

Törnqvist R, Jarsjö J. 2012. Water savings through improved irrigation techniques: basin-scale quantification in semi-arid environments. Water Resour. Manage., **26**: 949-962.

Törnqvist R, Jarsjö J, Karimov B. 2011. Health risks from large-scale water pollution: trends in Central Asia. Environment international, **37**: 435-442.

Törnqvist R, Jarsjö J, Thorslund J, Rao PSC, Basu NB, Destouni G. 2015. Mechanisms of basin-scale nitrogen load reductions under intensified irrigated agriculture. PloS one, **10**: e0120015.

Turner B, Meyer WB, Skole DL. 1994. Global land-use/land-cover change: towards an integrated study. Ambio. Stockholm, **23**: 91-95.

Uchida T, Asano Y, Mizuyama T, McDonnell JJ. 2004. Role of upslope soil pore pressure on lateral subsurface storm flow dynamics. Water Resour. Res., **40**.

Uchida T, Asano Y, Mizuyama T, McDonnell JJ. 2004. Role of upslope soil pore pressure on lateral subsurface storm flow dynamics. Water Resources Research, **40**: W12401. DOI: 10.1029/2003WR002139.

Uchida T, Kosugi K, Mizuyama T. 1999. Runoff characteristics of pipeflow and effects of pipeflow on rainfall-runoff phenomena in a mountainous watershed. J. Hydrol., **222**: 18-36. DOI: http://dx.doi.org/10.1016/S0022-1694(99)00090-6.

Uchida T, Kosugi Ki, Mizuyama T. 2001. Effects of pipeflow on hydrological process and its relation to landslide: a review of pipeflow studies in forested headwater catchments. Hydrol. Processes, **15**: 2151-2174.

Uhlenbrook S. 2006. Catchment hydrology—a science in which all processes are preferential. Hydrological Processes, **20**: 3581-3585. DOI: 10.1002/hyp.6564.

van Genuchten M, Naveira-Cotta C, Skaggs T, Raoof A, Pontedeiro E. 2014. The Use of Numerical Flow and Transport Models in Environmental Analyses. In: Application of Soil Physics in Environmental Analyses, Teixeira WG, Ceddia MB, Ottoni MV, Donnagema GK (eds.) Springer International Publishing, pp: 349-376.

Venot J-P, Molle F. 2008. Groundwater depletion in the Jordan highlands: can pricing policies regulate irrigation water use? Water Resour. Manage., **22**: 1925-1941.

Vertessy R, Benyon R, O'sullivan S, Gribben P. 1995. Relationships between stem diameter, sapwood area, leaf area and transpiration in a young mountain ash forest. Tree physiology, **15**: 559-567.

Vitousek PM, Gosz JR, Grier CC, Melillo JM, Reiners WA, Todd RL. 1979. Nitrate losses from disturbed ecosystems. Science, **204**: 469-474.

Voldoire A, Sanchez-Gomez E, y Mélia DS, Decharme B, Cassou C, Sénési S, Valcke S, Beau I, Alias A, Chevallier M. 2013. The CNRM-CM5. 1 global climate model: description and basic evaluation. Clim. Dyn., **40**: 2091-2121.

Walker BH, Abel N, Anderies JM, Ryan P. 2009. Resilience, adaptability, and transformability in the Goulburn-Broken Catchment, Australia. Ecology and society, **14**.

Wang Z, Feyen J, van Genuchten MT, Nielsen DR. 1998. Air entrapment effects on infiltration rate and flow instability. Water Resources Research, **34**: 213-222. DOI: 10.1029/97wr02804.

Waswa GW, Clulow AD, Freese C, Le Roux PAL, Lorentz SA. 2013. Transient Pressure Waves in the Vadose Zone and the Rapid Water Table Response. gsvadzone, **12**: -. DOI: 10.2136/vzj2012.0054.

Weeks EP. 2002. The Lisse Effect Revisited. Ground Water, **40**: 652-656. DOI: 10.1111/j.1745-6584.2002.tb02552.x.

Weiler M, McDonnell J. 2004. Virtual experiments: a new approach for improving process conceptualization in hillslope hydrology. J. Hydrol., **285**: 3-18. DOI: http://dx.doi.org/10.1016/S0022-1694(03)00271-3.

Weiler M, McDonnell JJ. 2007. Conceptualizing lateral preferential flow and flow networks and simulating the effects on gauged and ungauged hillslopes. Water Resour. Res., **43**: W03403. DOI: 10.1029/2006WR004867.

Weiler M, McDonnell JJ, Tromp-van Meerveld I, Uchida T. 2006. Subsurface Stormflow. In: Encyclopedia of Hydrological Sciences, John Wiley & Sons, Ltd.

Weiler M, McGlynn BL, McGuire KJ, McDonnell JJ. 2003. How does rainfall become runoff? A combined tracer and runoff transfer function approach. Water Resour. Res., **39**: 1315. DOI: 10.1029/2003WR002331.

Williams AP, Allen CD, Macalady AK, Griffin D, Woodhouse CA, Meko DM, Swetnam TW, Rauscher SA, Seager R, Grissino-Mayer HD. 2013. Temperature as a potent driver of regional forest drought stress and tree mortality. Nature Climate Change, **3**: 292-297.

Wilson GV, Jardine PM, Luxmoore RJ, Jones JR. 1990. Hydrology of a forested hillslope during storm events. Geoderma, **46**: 119-138. DOI: http://dx.doi.org/10.1016/0016-7061(90)90011-W.

Xiong Y, D'Atri JJ, Fu S, Xia H, Seastedt TR. 2011. Rapid soil organic matter loss from forest dieback in a subalpine coniferous ecosystem. Soil Biology and Biochemistry, **43**: 2450-2456.

Zabaleta A, Antigüedad I. 2013. Streamflow response of a small forested catchment on different timescales. Hydrol. Earth Syst. Sci., **17**: 211-223. DOI: 10.5194/hess-17-211-2013.

Zalewski M. 2002. Ecohydrology—the use of ecological and hydrological processes for sustainable management of water resources / Ecohydrologie—la prise en compte de processus écologiques et hydrologiques pour la gestion durable des ressources en eau. Hydrological Sciences Journal, **47**: 823-832. DOI: 10.1080/02626660209492986.

Zehe E, Blume T, Blöschl G. 2010. The principle of 'maximum energy dissipation': a novel thermodynamic perspective on rapid water flow in connected soil structures. Philosophical Transactions of the Royal Society B: Biological Sciences, **365**: 1377-1386. DOI: 10.1098/rstb.2009.0308.

Zhang M, Wei X. 2012. The effects of cumulative forest disturbance on streamflow in a large watershed in the central interior of British Columbia, Canada. Hydrol. Earth Syst. Sci., **16**: 2021-2034. DOI: 10.5194/hess-16-2021-2012.

Zhao R-J. 1992. The Xinanjiang model applied in China. J. Hydrol., **135**: 371-381.

Zhao R-J, Liu X, Singh V. 1995. The Xinanjiang model. Computer models of watershed hydrology.: 215-232.

Zhou MC, Ishidaira H, Hapuarachchi HP, Magome J, Kiem AS, Takeuchi K. 2006. Estimating potential evapotranspiration using Shuttleworth–Wallace model and NOAA-AVHRR NDVI data to feed a distributed hydrological model over the Mekong River basin. Journal of Hydrology, **327**: 151-173. DOI: http://dx.doi.org/10.1016/j.jhydrol.2005.11.013.

9. ORIGINAL PAPERS FOR THE THESIS

All 7 below listed scientific papers are based on the original findings, which were used for structuring the thesis.

Paper I. Langhammer, J., Su, Y., and Kaiglová, J., 2015. Runoff Response to Climate Warming and Forest Disturbance in a Mid-Mountain Basin. *Water*, 7, 3320-3342. DOI:10.3390/w7073320

Paper II. Jarsjo, J., Törnqvist, R., and Su, Y., 2017. Climate-driven change of nitrogen retention–attenuation near irrigated fields: multi-model projections for Central Asia. *Environmental Earth Sciences*, 76, 117. DOI:10.1007/s12665-017-6418-y

Paper III. Su Y., Langhammer, J., and Jarsjo, J., 2017. Geochemical responses of forested catchments to bark beetle infestation: Evidence from high frequency in-stream electrical conductivity monitoring. *Journal of Hydrology*, 550, 635-649. DOI:10.1016/j.jhydrol.2017.05.035

Paper IV. Shao, W., Su, Y.*, Yang Z., Ma, X., and Langhammer, J., 2018. Quantify the pore water velocity distribution by a celerity function. *Geofluids*, 2018, 19. DOI:10.1155/2018/1054730.

Paper V. Shao, W., Su, Y., and Langhammer, J., 2017. Simulations of coupled non-isothermal soil moisture transport and evaporation fluxes in a forest area. *Journal of hydrology and hydromechanics*, 66, 1-6. DOI: 10.1515/johh-2017-0038

Paper VI. Shao, W., Coenders-Gerrits, M., Judge, J., Zeng, Y., Su, Y.*, 2018. Simulation of non-isothermal soil moisture transport and evaporation fluxes in a maize cropland. *Journal of Hydrology*, 561, 833-847. DOI: 10.1016/j.jhydrol.2018.04.033.

Paper VII. Su, Y. *, Shao, W., Vlcek, L. and Langhammer, J., 2019. Ecohydrological Behaviour of Mountain Beech Forest: Quantification of Stomatal Conductance Using Sap Flow Measurements. Geosciences, 9(5), 243; DOI: 10.3390/geosciences9050243.